COMMUN. MATH. SCI.
Vol. 16, No. 7, pp. 1975–2002

DETECTION OF CONDUCTIVITY INCLUSIONS IN A SEMILINEAR ELLIPTIC PROBLEM ARISING FROM CARDIAC ELECTROPHYSIOLOGY*

ELENA BERETTA†, LUCA RATTI‡, AND MARCO VERANI§

Abstract. In this work we tackle the reconstruction of discontinuous coefficients in a semilinear elliptic equation from the knowledge of the solution on the boundary of the planar bounded domain. The problem is motivated by an application in cardiac electrophysiology.

We formulate a constraint minimization problem involving a quadratic mismatch functional enhanced with a regularization term which penalizes the perimeter of the inclusion to be identified. We introduce a phase-field relaxation of the problem, employing a Ginzburg-Landau-type energy and assessing the Γ-convergence of the relaxed functional to the original one. After computing the optimality conditions of the phase-field optimization problem and introducing a discrete finite element formulation, we propose an iterative algorithm and prove convergence properties. Several numerical results are reported, assessing the effectiveness and the robustness of the algorithm in identifying arbitrarily-shaped inclusions.

Finally, we compare our approach to a shape derivative based technique, both from a theoretical point of view (computing the sharp interface limit of the optimality conditions) and from a numerical one.

Keywords. inverse problem; semilinear elliptic equation; phase-field relaxation.

AMS subject classifications. 65N21; 35J61; 35R30.

1. Introduction

We consider the following Neumann problem, defined over $\Omega\subset\mathbb{R}^2$:

$$\begin{cases} -\mathrm{div}(\tilde{k}(x)\nabla y)+\chi_{\Omega\setminus\omega}y^3=f & \text{in } \Omega \\ \partial_\nu y=0 & \text{on } \partial\Omega, \end{cases} \tag{1.1}$$

where $\chi_{\Omega\setminus\omega}$ is the indicator function of $\Omega\setminus\omega$ and

$$\tilde{k}(x)=\begin{cases} k \text{ if } x\in\omega \\ 1 \text{ if } x\in\Omega\setminus\omega, \end{cases}$$

with $0<k\ll 1$ and $f\in L^2(\Omega)$.

The boundary value problem (1.1) consists of a semilinear diffusion-reaction equation with discontinuous coefficients across the interface of an inclusion $\omega\subset\Omega$, in which the conducting properties are different from the background medium. Supposing the value of k to be known, our goal is the determination of the inclusion from the knowledge of the value of y on the boundary $\partial\Omega$. More precisely, given the measured data y_{meas} on the boundary, we search for the inclusion $\omega\subset\Omega$ that is associated with those exact measurements, i.e. such that the corresponding solution y of (1.1) satisfies

$$y|_{\partial\Omega}=y_{meas}. \tag{1.2}$$

*Received: January 31, 2018; Accepted (in revised form): July 12, 2018. Communicated by Liliana Borcea.

†Dipartimento di Matematica, Politecnico di Milano, P.za Leonardo da Vinci 32, 20133 Milano, Italy (elena.beretta@polimi.it).

‡Dipartimento di Matematica, Politecnico di Milano, P.za Leonardo da Vinci 32, 20133 Milano, Italy (luca.ratti@polimi.it).

§Dipartimento di Matematica, Politecnico di Milano, P.za Leonardo da Vinci 32, 20133 Milano, Italy (marco.verani@polimi.it).

Since, to the best of our knowledge, few works deal with inverse boundary value problems for nonlinear equations, the reconstruction problem analyzed in this paper is interesting from both an analytic and a numerical standpoint.

The direct problem can be related to a meaningful application arising in cardiac electrophysiology: in that context (see [19, 39]), the solution y represents the electric transmembrane potential in the heart tissue, the coefficient $\tilde{k}$ is the tissue conductivity and the nonlinear reaction term encodes an ionic transmembrane current. An inclusion ω models the presence of an ischemia, which modifies substantially the conductivity properties of the tissue. The objective of our work, in the long run, is the identification of ischemic regions through a set of measurements of the electric potential acquired on the surface of the myocardium. We remark that our model is a simplified version of the more complex *monodomain* model (see e.g. [39, 40]). The monodomain is a continuum model which describes the evolution of the transmembrane potential on the heart tissue according to the conservation law for currents and a satisfying description of the ionic current, which entails the coupling with a system of ordinary differential equations for the concentration of chemical species. In this preliminary setting, we remove the coupling with the ionic model, adopting instead a phenomenological description of the ionic current, through the introduction of a cubic reaction term. Moreover, we consider the stationary case in presence of a source term which plays the role of the electrical stimulus. Despite the simplifications, the problem we consider in this paper is a mathematical challenge in itself. Indeed, here the difficulties include the nonlinearity of both the direct and the inverse problem, as well as the lack of measurements at our disposal.

The linear counterpart of the problem, obtained when the nonlinear reaction term is removed, is strictly related to the *inverse conductivity problem*, also called *Calderón problem*, which has been the object of several studies in the last decades. The problem is severly ill-posed and highly nonlinear. Moreover, infinite measurements are needed to recover smooth inclusions (see [30] and references therein). A finite number of measurements is sufficient to determine uniquely and in a stable (Lipschitz) way the inclusion, only after introducing additional information either on the shape of the inclusion or on its size.

Several reconstruction algorithms have been developed for the solution of the inverse conductivity problem, and it is beyond the purposes of this introduction to provide an exhaustive overview on the topic. Under the assumption that the inclusion to be reconstructed is of small size, an extended review of methods is presented in [4], many of which heavily rely on the linearity of the direct problem. Some efficient and more versatile algorithms can be derived by a variational approach, i.e., by the constraint minimization of a quadratic misfit functional, as in [31], and [3]. When dealing with the reconstruction of arbitrary inclusions in the linear case, several variational algorithms are available. A shape-optimization approach, with suitable regularization, is explored in [1, 28, 32] and [2]; in [29] this approach is coupled with topology optimization; whereas the level set technique has been applied in [38] and in [13]. Recently, several specific schemes have been employed to deal with the minimization of a misfit functional endowed with a total-variation regularization: along this line we mention the Levenberg-Marquardt and Landweber algorithms in [5], the augmented Lagrangian approach in [17] and the regularized level set technique in [15]. Finally, the phase-field approach has been explored for the linear inverse conductivity problem e.g in [37] and recently in [20].

Concerning inverse problems related to nonlinear PDEs, only a few theoretical results and numerical strategies are available, especially regarding the electrophysiological problem of interest. We remark that the level-set method has been implemented for the reconstruction of extended inclusions in the nonlinear problem of cardiac electrophysiology (see [34] and [16]), by evaluating the sensitivity of the cost functional with respect to a selected set of parameters involved in the full discretization of the shape of the inclusion. In [10], the authors, taking advantage from the results obtained in [8], proposed a reconstruction algorithm for the nonlinear problem (1.1) based on topological optimization, where a suitable quadratic functional is minimized to detect the position of *small* inclusions *separated* from the boundary. In [7], the results obtained in [10] and [8] have been extended to the time-dependent monodomain equation under the same assumptions.

In this paper we propose a reconstruction algorithm of inclusions of *arbitrary* shape and position by relying on the minimization of a suitable functional, enhanced with a perimeter penalization term, and by following a relaxation strategy relying on the phase-field approach. The outline of the paper is as follows. In Section 2 we introduce the optimization problem together with its phase-field regularization, discussing well-posedness, Γ-convergence of the relaxed functional to the original one, and the derivation of necessary optimality conditions associated with the phase-field minimization problem. In Section 3 we propose an iterative reconstruction algorithm allowing for the numerical approximation of the solution and prove its convergence properties. The power of this approach is twofold. On the one hand it allows to consider conductivity inclusions of arbitrary shape and position, which is the case of interest for our application and on the other it leads to good reconstructions as shown in the numerical experiments in Section 4. Finally, in Section 5 we compare our technique with a shape optimization based approach. After showing that the optimality conditions derived for the relaxed problem converge to those corresponding to the sharp interface one, we show numerical results obtained by applying both the algorithms on the same benchmark cases.

2. Minimization problem

In this section, we give a rigorous formulation both of the direct and of the inverse problem under investigation. The analysis of the well-posedness of the direct problem is reported in detail, and consists of an extension of the results previously obtained in [8]. The inverse problem is instead associated with a constraint minimization problem for which we introduce a regularization and relaxation strategy in order to overcome instability and to allow the implementation of a reconstruction algorithm.

We formulate the problems (1.1) and (1.2) in terms of the indicator function of the inclusion, $u=\chi_\omega$. We assume an *a priori* hypothesis on the inclusion, namely that it is a subset of Ω of finite perimeter: u belongs to $BV(\Omega)=\{v\in L^1(\Omega):\ TV(v)<\infty\}$, with

$$TV(v)=\sup\left\{\int_\Omega v\mathrm{div}(\phi);\quad \phi\in C_0^1(\Omega;\mathbb{R}^2),\ \|\phi\|_{L^\infty}\le 1\right\},$$

endowed with the norm $\|\cdot\|_{BV}=\|\cdot\|_{L^1}+TV(\cdot)$. Moreover, we formulate particular restrictions on the inclusion and on the source f.

Assumption 2.1. *Given a positive number d_0 we assume that*

$$u\in X_{0,1}=\{v\in BV(\Omega):v(x)\in\{0,1\}\ a.e.\ in\ \Omega\ ,u=0\ a.e.\ in\ \Omega^{d_0}\ \}, \tag{2.1}$$

where $\Omega^{d_0}=\{x\ s.t.\ dist(x,\partial\Omega)\le d_0\}$.

This also entails that the inclusion is well separated from the boundary $\partial\Omega$. Moreover, Assumption 2.2. *Given a positive constant m, we require*

$$f \geq m \quad a.e. \ in \ \Omega. \tag{2.2}$$

The weak formulation of the direct problem (1.1) in terms of u reads: find y in $H^1(\Omega)$ s.t., $\forall \varphi \in H^1(\Omega)$,

$$\int_\Omega a(u)\nabla y \nabla \varphi + \int_\Omega b(u) y^3 \varphi = \int_\Omega f\varphi, \tag{2.3}$$

being $a(u)=1-(1-k)u$ and $b(u)=1-u$. Define $S: X_{0,1} \to H^1(\Omega)$ the *solution map*: for all $u \in X_{0,1}$, $S(u)=y$ is the solution to problem (2.3) with indicator function u; the inverse problem consists of:

$$\textit{find } u \in X_{0,1} \ \textit{s.t.} \ S(u)|_{\partial\Omega} = y_{meas}. \tag{2.4}$$

In the proof of various propositions, we have to make use of the following generalized Poincaré inequality:

Lemma 2.1. $\exists C>0, C=C(\Omega,d_0)$ *s.t.*, $\forall w \in H^1(\Omega)$,

$$\|w\|^2_{H^1(\Omega)} \leq C\left(\|\nabla w\|^2_{L^2(\Omega)} + \|w\|^2_{L^2(\Omega^{d_0})}\right). \tag{2.5}$$

The proof of the Lemma 2.1 is given in the Appendix of [8] and easily follows from Theorem 8.11 in [33].

Thanks to Lemma 2.1, we can prove the following well-posedness result for the direct problem.

Proposition 2.1. *Consider $f \in \left(H^1(\Omega)\right)^*$ and a function $u \in X_{0,1}$. Then there exists a unique solution $S(u) \in H^1(\Omega)$ of*

$$\int_\Omega a(u)\nabla S(u)\cdot\nabla v + \int_\Omega b(u)S(u)^3 v = \int_\Omega f v \qquad \forall v \in H^1(\Omega),$$

where $a(u)=1-(1-k)u$ and $b(u)=1-u$.

Proof. The proof is analogous to the analysis performed in [8, Theorem 4.1], but generalises that result to the case of inclusions of finite perimeter. The strategy consists in applying the Minty-Browder theorem on the direct operator $T: H^1(\Omega) \to \left(H^1(\Omega)\right)^*$ s.t.

$$\langle T(S), v\rangle_* = \int_\Omega a(u)\nabla S\cdot\nabla v + \int_\Omega b(u)S^3 v,$$

which shows to be continuous, coercive and strictly monotone. In particular

- Local Lipschitz continuity:

$$\begin{aligned}|\langle T(S)-T(S_0), v\rangle_*| &= \left|\int_\Omega a(u)\nabla(S-S_0)\cdot\nabla v + \int_\Omega b(u)(S-S_0)qv\right| \\ &\leq \|\nabla(S-S_0)\|_{L^2}\|\nabla v\|_{L^2} + \|S-S_0\|_{L^6}\|q\|_{L^3}\|v\|_{L^2},\end{aligned}$$

  (with $q=S^2+SS_0+S_0^2$). If S and S_0 belong to a bounded subset of $H^1(\Omega)$, then (thanks to the Sobolev embedding of $H^1(\Omega)$ in $L^6(\Omega)$) we can assess that $\|q\|_{L^3} \leq M$ and moreover $\exists K=K(u)>0$ s.t.

$$|\langle T(S)-T(S_0), v\rangle_*| \leq K\|S-S_0\|_{H^1}\|v\|_{H^1} \qquad \forall v \in H^1(\Omega).$$

- Coercivity: We show that $\langle T(S),S\rangle_* \to +\infty$ as $\|S\|_{H^1(\Omega)} \to +\infty$. Since $u=0$ a.e. in Ω^{d_0}, $b(u) \geq \chi_{\Omega^{d_0}}$, the indicator function of Ω^{d_0}. Then,

$$\langle T(S),S\rangle_* \geq k\int_\Omega |\nabla S|^2 + \int_{\Omega^{d_0}} S^4 \geq k\|\nabla S\|^2_{L^2(\Omega)} + \frac{1}{|\Omega|}\|S\|^4_{L^2(\Omega^{d_0})}$$
$$= k\left(\|\nabla S\|^2_{L^2(\Omega)} + \|S\|^2_{L^2(\Omega^{d_0})}\right) + R,$$

where $R = \frac{1}{|\Omega|}\|S\|^4_{L^2(\Omega^{d_0})} - k\|S\|^2_{L^2(\Omega^{d_0})}$ can be bounded by below independently of S: $R \geq -\frac{k^2|\Omega|}{4}$. Together with Poincaré's inequality in Lemma 2.1, we conclude that

$$\langle T(S),S\rangle_* \geq \frac{k}{C}\|S\|^2_{H^1(\Omega)} - \frac{k^2|\Omega|}{4}.$$

- (Strict) monotonicity: We claim that $\langle T(S)-T(R),S-R\rangle_* \geq 0$ and $\langle T(S)-T(R),S-R\rangle_* = 0 \Leftrightarrow S=R$. Indeed,

$$\langle T(S)-T(R),S-R\rangle_* \geq \int_\Omega k|\nabla(S-R)|^2 + \int_{\Omega^{d_0}} (S^2+SR+R^2)(S-R)^2 \geq 0.$$

Moreover, since $S^2+SR+R^2 \geq \frac{1}{4}(S-R)^2$,

$$\langle T(S)-T(R),S-R\rangle_* = 0 \Rightarrow \|\nabla(S-R)\|_{L^2(\Omega)} = 0 \text{ and } \int_{\Omega^{d_0}} (S-R)^4 = 0,$$

and from the latter equality it follows that $S=R$ a.e. in Ω^{d_0}, hence also $\|S-R\|_{L^2(\Omega^{d_0})} = 0$, and via Lemma 2.1 $\|S-R\|_{H^1(\Omega)} = 0$.

□

It is possible to prove additional properties of the solution $S(u)$ of the direct problem. In particular, we provide a uniform bound on $\|S(u)\|_{H^1(\Omega)}$ independent of u.

PROPOSITION 2.2. *There exists a constant $C = C(\Omega,d_0,k)$ s.t., $\forall u \in X_{0,1}$,*

$$\|S(u)\|_{H^1(\Omega)} \leq C\left(\|f\|_{L^2(\Omega)} + \|f\|^3_{L^2(\Omega)}\right). \tag{2.6}$$

This can be proved as in [8, Proposition 4.1], where we take advantage of the bound

$$\|S(u)\|^4_{L^2(\Omega^{d_0})} \leq |\Omega^{d_0}|\int_{\Omega^{d_0}} S(u)^4 \leq |\Omega|\int_\Omega b(u)S(u)^4,$$

and hence the constant appearing in (2.6) only depends on Ω, d_0, k.

Moreover, we prove a Hölder regularity result on $S(u)$:

PROPOSITION 2.3. *Let $S(u)$ be the solution of* (2.3) *associated to $u \in X_{0,1}$ and let $f \in L^2(\Omega)$. Then, $S(u) \in C^\alpha(\bar\Omega)$ and*

$$\|S(u)\|_{C^\alpha(\bar\Omega)} \leq C(\Omega,k,\|f\|_{L^2(\Omega)},d_0).$$

Proof. The proof is analogous to the one in [8]. An application of [26, Theorem 8.24] ensures that

$$\forall \Omega' \subset\subset \Omega, \quad \|S(u)\|_{C^\alpha(\overline{\Omega'})} \leq C\left(\|S(u)\|_{L^2(\Omega)} + \|S(u)\|^3_{L^6(\Omega)} + \|f\|_{L^2(\Omega)}\right) \leq C,$$

where $C = C(\overline{\Omega'}, k, \|f\|_{L^2(\Omega)})$. By taking $\Omega' \supset \Omega^{d_0}$, since the conductivity is constant in Ω_{d_0} and the normal derivative on the boundary is zero, we can apply standard regularity results up to the boundary, obtaining:

$$\|S(u)\|_{C^\alpha(\overline{\Omega})} \leq C = C(\Omega, d_0, k, \|f\|_{L^2(\Omega)}).$$

∎

Finally, we prove an estimate which occurs many times in the proof of various results.

PROPOSITION 2.4. *Suppose that $f \in L^2(\Omega)$ s.t. $f \geq m > 0$ a.e. in Ω. Consider $S(u)$ to be the solution of problem* (2.3) *associated with $u \in X_{0,1}$. Then, $S(u) \geq m^{1/3}$.*

The proof is an immediate consequence of the following Lemma:

LEMMA 2.2. *Let S_1 and S_2 be a sub- and supersolution of* (2.3) *with $u \in X_{0,1}$, namely $S_1, S_2 \in H^1(\Omega)$ s.t., $\forall \varphi \in H^1(\Omega)$, $\varphi \geq 0$ a.e., it holds:*

$$\int_\Omega a(u) \nabla S_1 \cdot \nabla \varphi + \int_\Omega b(u) S_1^3 \varphi - \int_\Omega f \varphi \leq 0, \tag{2.7}$$

$$\int_\Omega a(u) \nabla S_2 \cdot \nabla \varphi + \int_\Omega b(u) S_2^3 \varphi - \int_\Omega f \varphi \geq 0. \tag{2.8}$$

Then, $S_1 \leq S_2$ a.e. in Ω.

Proof. Subtract the Equations (2.8) – (2.7) and define $W = S_2 - S_1$: it holds that $\forall \varphi \in H^1(\Omega)$, $\varphi \geq 0$ a.e.,

$$\int_\Omega a(u) \nabla W \cdot \nabla \varphi + \int_\Omega b(u) Q W \varphi \geq 0,$$

where $Q = (S_1^2 + S_1 S_2 + S_2^2) \geq 0$. Take $\varphi = W^-$, the negative part of W. We remark that $W^+ = max\{0, W\}$, $W^- = max\{0, -W\}$, $W = W^+ - W^-$; moreover $W^+, W^- \in H^1(\Omega)$, $W^+ W^- = 0$, and in view of [24, Theorem 4.4] we refer to ∇W^- as the gradient of the negative part W^- or equivalently as the vector of the negative parts of the components of ∇W. Thus, it holds that

$$\int_\Omega a(u) \nabla W^- \cdot \nabla W^- + \int_\Omega b(u) Q (W^-)^2 \leq 0,$$

which implies that $S_2 \geq S_1$ *a.e.* Indeed, $k\|\nabla W^-\|_{L^2(\Omega)} \leq 0$ implies $\nabla W^- = 0$ a.e. in Ω; moreover, both S_1 and S_2 are continuous, and hence also W and W^-, which entails $W^- = c$, $c \geq 0$ by definition. In order to guarantee that $W^- = max\{0, -W\} = c$ is continuous, either $c = 0$ or $W = -c < 0$ in Ω. The latter case, though, would imply that $S_2 = S_1 - c$ and, by simple computation, $Q = 3S_1^2 - 3cS_1 + c^2 \geq \frac{c^2}{4}$, which is incompatible with $\int_\Omega b(u) Q (W^-)^2 \leq 0$. Hence $W^- = 0$, and so $W = W^+ \geq 0$. ∎

Proof. **(Proof of Proposition 2.4.)** Taking $S_2 = S(u)$ and $S_1 = m^{1/3}$ (which is a subsolution since $b(u)m - f \leq 0$), we obtain the uniform bound $S(u) \geq m^{1/3}$. ∎

REMARK 2.1. We could extend all the previous results to a class of more general functions f, namely f not vanishing in Ω^{d_0}, but that would entail that the lower bound in Proposition 2.4 might depend on u. On the other hand, when applying the previous estimates in the proofs of following results (in particular, Propositions 2.5, 2.10, 5.1 and Lemma 3.1), we always invoke Proposition 2.4 on a fixed indicator function u.

The crucial property satisfied by the solution map is the continuity with respect to the L^1 norm, which requires an accurate treatment due to the nonlinearity of the direct problem.

PROPOSITION 2.5. *Let $f \in L^2(\Omega)$ satisfy Assumption* (2.2). *If $\{u_n\} \subset X_{0,1}$ s.t. $u_n \xrightarrow{L^1} u \in X_{0,1}$, then $S(u_n)|_{\partial\Omega} \xrightarrow{L^2(\partial\Omega)} S(u)|_{\partial\Omega}$.*

Proof. Define $w_n = S(u_n) - S(u)$; then, subtracting (2.3) evaluated at u_n and the same evaluated at u; w_n is the solution of:

$$\int_\Omega a(u_n)\nabla w_n \nabla\varphi + \int_\Omega b(u_n) q_n w_n \varphi = \int_\Omega (1-k)(u_n - u)\nabla S(u)\nabla\varphi - \int_\Omega (u_n - u) S(u)^3 \varphi, \tag{2.9}$$

where $q_n = S(u_n)^2 + S(u_n)S(u) + S(u)^2$. Considering $\varphi = w_n$ and taking advantage of the fact that $a(u_n) \geq k$ and (by simple computation) $q_n \geq \frac{3}{4}S(u)^2$, we can show, via the Cauchy-Schwarz inequality, that

$$k\|\nabla w_n\|^2_{L^2(\Omega)} + \frac{3}{4}\int_\Omega b(u_n)S(u)^2 w_n^2 \leq (1-k)\|(u_n-u)\nabla S(u)\|_{L^2(\Omega)}\|\nabla w_n\|_{L^2(\Omega)} + \left\|(u_n-u)S(u)^3\right\|_{L^2(\Omega)}\|w_n\|_{L^2(\Omega)}.$$

We remark that $(u_n - u)S(u)^3 \in L^2(\Omega)$ since $S(u) \in H^1(\Omega) \subset\subset L^6(\Omega)$. Moreover, as $b(u_n) \geq \chi_{\Omega^{d_0}}$ and using Proposition 2.4,

$$k\|\nabla w_n\|^2_{L^2(\Omega)} + \frac{3}{4}\int_{\Omega^{d_0}} m^{2/3} w_n^2 \leq (1-k)\|(u_n-u)\nabla S(u)\|_{L^2(\Omega)}\|\nabla w_n\|_{L^2(\Omega)} + \left\|(u_n-u)S(u)^3\right\|_{L^2(\Omega)}\|w_n\|_{L^2(\Omega)},$$

from which we deduce

$$k\|\nabla w_n\|^2_{L^2(\Omega)} + \frac{3}{4}m^{2/3}\|w_n\|^2_{L^2(\Omega^{d_0})} \leq (q_1 + q_2)\|w_n\|_{H^1(\Omega)},$$

where $q_1 = \|(u_n - u)\nabla S(u)\|_{L^2(\Omega)}$ and $q_2 = \left\|(u_n-u)S(u)^3\right\|_{L^2(\Omega)}$, which implies, thanks to the Poincaré inequality in Lemma 2.1,

$$\|w_n\|_{H^1(\Omega)} \leq C(q_1 + q_2),$$

with $C = C(d_0, \Omega, m, k)$. Consider

$$q_1 = \left(\int_\Omega (u_n - u)^2 |\nabla S(u)|^2\right)^{\frac{1}{2}};$$

since $u_n \xrightarrow{L^1} u$, then (up to a subsequence) $u_n \to u$ pointwise almost everywhere. Thus also the integrand $(u_n - u)^2|\nabla S(u)|^2$ converges to 0. Moreover, $|u_n - u| \leq 1$, hence $\forall n$ $(u_n - u)^2|\nabla S(u)|^2 \leq |\nabla S(u)|^2 \in L^1(\Omega)$, and thanks to Lebesgue convergence theorem, we conclude that $q_1 \to 0$. Analogously, $q_2 \to 0$ and eventually $\|w_n\|_{H^1(\Omega)} \to 0$, i.e. $S(u_n) \xrightarrow{H^1} S(u)$ and by the trace inequality also $S(u_n)|_{\partial\Omega} \xrightarrow{L^2(\partial\Omega)} S(u)|_{\partial\Omega}$. ∎

REMARK 2.2. $X_{0,1}$, being a closed subspace of the Banach space $BV(\Omega)$, is compact with respect to its weak topology; moreover, the weak BV convergence implies the strong

L^1 convergence, and in view of Proposition 2.5 we can assess that the map $F=\tau\circ S$, τ being the trace operator in $H^1(\Omega)$, is compact from $X_{0,1}$ to $L^2(\partial\Omega)$. It is immediate to conclude that, if the inverse F^{-1} exists, it cannot be continuous: hence, the inverse problem (2.4) is ill-posed.

We now introduce the following constraint optimization problem:

$$\underset{u\in X_{0,1}}{\arg\min}\, J(u); \qquad J(u)=\frac{1}{2}\|S(u)-y_{meas}\|^2_{L^2(\partial\Omega)}, \tag{2.10}$$

which shares the same property of non-stability and (possibly) non-uniqueness as problem (2.4). Nevertheless, a well-known strategy to recover well-posedness for problem (2.10) is to introduce a Tikhonov regularization term in the functional to minimize, e.g. a penalization term for the perimeter of the inclusion. The regularized problem reads:

$$\underset{u\in X_{0,1}}{\arg\min}\, J_{reg}(u); \quad J_{reg}(u)=\frac{1}{2}\|S(u)-y_{meas}\|^2_{L^2(\partial\Omega)}+\alpha TV(u), \tag{2.11}$$

For the regularized problem (2.11), it is possible to prove several desirable properties:

- for every $\alpha>0$ there exists at least one solution to (2.11) (existence);
- small perturbations on the data y_{meas} in $L^2(\partial\Omega)$-norm imply small perturbation on the solutions of (2.11) in BV-intermediate convergence (stability);
- the sequence of solutions of problem (2.11) associated with the regularization parameters $\{\alpha_k\}$ (s.t. $\alpha_k\to 0$) converges in the BV-intermediate convergence to a minimum-variation solution of problem (2.10).

We point out that a sequence $\{u_n\}\subset BV(\Omega)$ converges to $u\in BV(\Omega)$ in the sense of the intermediate convergence iff $u_n\xrightarrow{L^1}u$ and $TV(u_n)\to TV(u)$. The proof of the previous properties follows from a careful application of the results in [23, Chapter 10], taking into account that $BV(\Omega)$ is a non-reflexive Banach space.

According to the stated results, a good approximation of a minimum-variation solution of the inverse problem (2.4) can be achieved by solving the regularized constraint minimization problem (2.11) with a sufficiently small parameter $\alpha>0$. Although the stability of the problem is guaranteed, its numerical solution may raise difficulties, namely the non-convexity both of the functional J_{reg} and of the space $X_{0,1}$, as well as the non-differentiability of the functional. To overcome these difficulties, in this work we propose a phase-field relaxation of the optimization problem (2.11) inspired by [20], with the additional difficulty of the nonlinearity of the direct problem. The relaxation strategy consists in defining a minimization problem in a space of more regular functions, associated to a differentiable cost functional (which in our case is achieved by replacing the total variation term with a Modica-Mortola functional, representing a Ginzburg-Landau energy).

Consider $u\in\mathcal{K}=\{v\in H^1(\Omega)\colon\ 0\le v\le 1 \textit{ a.e. in } \Omega,\ v=0 \textit{ a.e. in } \Omega^{d_0}\}$ and, for every $\varepsilon>0$, introduce the optimization problem:

$$\underset{u\in\mathcal{K}}{\arg\min}\, J_\varepsilon(u); \quad J_\varepsilon(u)=\frac{1}{2}\|S(u)-y_{meas}\|^2_{L^2(\partial\Omega)}+\alpha\int_\Omega\left(\varepsilon|\nabla u|^2+\frac{1}{\varepsilon}u(1-u)\right). \tag{2.12}$$

The well-posedness result for the direct problem in Proposition 2.1, together with the additional stability and regularity results can be easily extended to the case $u\in\mathcal{K}$. In the next two propositions, we prove existence and stability of the solutions of the relaxed minimization problem (2.12) for fixed ε.

PROPOSITION 2.6. *For every fixed $\varepsilon > 0$, the minimization problem* (2.12) *has a solution $u_\varepsilon \in \mathcal{K}$.*

Proof. Fix $\varepsilon > 0$ and consider a minimizing sequence for the functional J_ε, $\{u_k\} \subset \mathcal{K}$ (we omit the dependence of u_k on ε). By definition of minimizing sequence, $J_\varepsilon(u_k) \le M$ independently of k, which implies that $\|\nabla u_k\|^2_{L^2(\Omega)}$ is also bounded. Moreover, with $u_k \in \mathcal{K}$, $0 \le u_k \le 1$ a.e., thus $\|u_k\|_{L^2(\Omega)}$ and $\|u_k\|_{H^1(\Omega)}$ are bounded independently of k. Thanks to weak compactness of H^1, there exist $u_\varepsilon \in H^1(\Omega)$ and a subsequence $\{u_{k_n}\}$ s.t. $u_{k_n} \xrightarrow{H^1} u_\varepsilon$, hence $u_{k_n} \xrightarrow{L^2} u_\varepsilon$. The strong L^2 convergence implies (up to a subsequence) pointwise convergence a.e., which allows to conclude (together with the Lebesgue's dominated convergence theorem, since $u_{k_n}(1-u_{k_n}) \le 1/2$) that

$$\int_\Omega u_{k_n}(1-u_{k_n}) \to \int_\Omega u_\varepsilon(1-u_\varepsilon).$$

Moreover, by the lower semicontinuity of the H^1 norm with respect to the weak convergence, and by the compact embedding in L^2,

$$\begin{aligned}
\|u_\varepsilon\|^2_{H^1(\Omega)} &\le \liminf_n \|u_{k_n}\|^2_{H^1(\Omega)} \\
\|u_\varepsilon\|^2_{L^2(\Omega)} + \|\nabla u_\varepsilon\|^2_{L^2(\Omega)} &\le \lim_n \|u_{k_n}\|^2_{L^2(\Omega)} + \liminf_n \|\nabla u_{k_n}\|^2_{L^2(\Omega)} \\
\|\nabla u_\varepsilon\|^2_{L^2(\Omega)} &\le \liminf_n \|\nabla u_{k_n}\|^2_{L^2(\Omega)}.
\end{aligned}$$

Moreover, using the continuity of the solution map S with respect to the L^1 convergence, we can conclude that

$$J_\varepsilon(u_\varepsilon) \le \liminf_n J_\varepsilon(u_{k_n}).$$

Finally, by pointwise convergence, $0 \le u_\varepsilon \le 1$ a.e. and $u_\varepsilon = 0$ a.e. in Ω^{d_0}, hence u_ε is a minimum of J_ε in $\mathcal{K}$. ∎

PROPOSITION 2.7. *Fix $\alpha, \varepsilon > 0$ and consider a sequence $\{y^k\} \subset L^2(\partial\Omega)$ such that $y^k \xrightarrow{L^2(\partial\Omega)} y_{meas}$. For each k, let u^k_ε be a solution of* (2.12)*, where y_{meas} is replaced by y^k. Then, up to a subsequence, $u^k_\varepsilon \xrightarrow{H^1} u_\varepsilon$, where u_ε is a solution of* (2.12).

Proof. Consider a solution u^* of (2.12): by definition of u^k_ε, it holds

$$\begin{aligned}
&\frac{1}{2}\left\|S(u^k_\varepsilon) - y^k\right\|^2_{L^2(\partial\Omega)} + \alpha\varepsilon\left\|\nabla u^k_\varepsilon\right\|^2_{L^2(\Omega)} + \frac{\alpha}{\varepsilon}\int_\Omega u^k_\varepsilon(1-u^k_\varepsilon) \\
\le &\frac{1}{2}\left\|S(u^*) - y^k\right\|^2_{L^2(\partial\Omega)} + \alpha\varepsilon\|\nabla u^*\|^2_{L^2(\Omega)} + \frac{\alpha}{\varepsilon}\int_\Omega u^*(1-u^*) \\
\le &\frac{1}{2}\left\|y_{meas} - y^k\right\|^2_{L^2(\partial\Omega)} + \frac{1}{2}J_\varepsilon(u^*).
\end{aligned}$$

Hence $\left\|\nabla u^k_\varepsilon\right\|_{L^2(\Omega)}$ is bounded independently of k, and so is $\left\|u^k_\varepsilon\right\|_{L^2(\Omega)}$ (since $u^k_\varepsilon \in \mathcal{K}$). This implies that, up to a subsequence, $u^k_\varepsilon \xrightarrow{H^1} u_\varepsilon \in H^1(\Omega)$, from which it follows that $u^k_\varepsilon \xrightarrow{L^2} u_\varepsilon$ and in particular $S(u^k_\varepsilon) \xrightarrow{H^1} S(u_\varepsilon)$ (thanks to Proposition 2.5) and $u^k_\varepsilon \to u_\varepsilon$ almost everywhere in Ω, and by Lebesgue's convergence theorem also $\int_\Omega u^k_\varepsilon(1-u^k_\varepsilon) \to$

$\int_\Omega u_\varepsilon(1-u_\varepsilon)$. Finally, by lower semicontinuity of the H^1 norm with respect to the weak convergence, we conclude that

$$J_\varepsilon(u_\varepsilon) \le \liminf_k \left(\frac{1}{2} \| S(u_\varepsilon^k) - y^k \|^2_{L^2(\partial\Omega)} + \alpha\varepsilon \| \nabla u_\varepsilon^k \|^2_{L^2(\Omega)} + \frac{\alpha}{\varepsilon} \int_\Omega u_\varepsilon^k (1-u_\varepsilon^k) \right)$$
$$\le J_\varepsilon(u^*) + \frac{1}{2} \lim_k \| y_{meas} - y^k \|^2_{L^2(\partial\Omega)},$$

hence $J_\varepsilon(u_\varepsilon) = J_\varepsilon(u^*)$ and u_ε is a solution of (2.12). Moreover, this implies that $\|\nabla u_\varepsilon\|_{L^2(\Omega)} = \lim_k \|\nabla u_\varepsilon^k\|_{L^2(\Omega)}$; and since H^1 is an Hilbert space, together with the weak convergence, this implies that $u_\varepsilon^k \xrightarrow{H^1} u_\varepsilon$. ∎

The asymptotic behaviour of the phase-field relaxation when $\varepsilon \to 0$ is reported in the next two propositions and is related to the notion of Γ-convergence.

PROPOSITION 2.8. *Consider the space X of the Lebesgue-measurable functions over Ω endowed with the $L^1(\Omega)$ norm and the following extension of the cost functionals on X*

$$\tilde{J} = \begin{cases} J_{reg}(u) & \text{if } u \in X_{0,1} \\ \infty & \text{otherwise,} \end{cases} \qquad \tilde{J}_\varepsilon = \begin{cases} J_\varepsilon(u) & \text{if } u \in \mathcal{K} \\ \infty & \text{otherwise.} \end{cases}$$

Then, the functionals $\tilde{J}_{\varepsilon_k}$ associated with $\{\varepsilon_k\}$ s.t. $\varepsilon_k \to 0$ converge to $\tilde{J}$ in X in the sense of the $\Gamma-$convergence.

The proof can be obtained by adapting the one of [20, Theorem 6.1]. Moreover, from the compactness result in [6, Proposition 4.1] and by the definition of Γ-convergence, it is easy to prove the following convergence result for the solutions of (2.12).

PROPOSITION 2.9. *Consider a sequence $\{\varepsilon_k\}$ s.t. $\varepsilon_k \to 0$ and let $\{u_{\varepsilon_k}\}$ be the sequence of the respective minimizers of the functionals $\{J_{\varepsilon_k}\}$. Then, there exists a subsequence, still denoted as $\{\varepsilon_k\}$ and a function $u \in X_{0,1}$ such that $u_{\varepsilon_k} \to u$ in L^1 and u is a solution of* (2.11).

2.1. Optimality conditions. We can now provide an expression for the optimality condition associated with the minimization problem (2.12), which is formulated as a variational inequality involving the Fréchet derivative of J_ε.

PROPOSITION 2.10. *Consider the solution map $S : \mathcal{K} \to H^1(\Omega)$ and let $f \in L^2(\Omega)$ satisfy Assumption* (2.2)*: for every $\varepsilon > 0$, the operators S and J_ε are Fréchet-differentiable on $\mathcal{K} \subset L^\infty(\Omega) \cap H^1(\Omega)$ and a minimizer u_ε of J_ε satisfies the variational inequality:*

$$J'_\varepsilon(u_\varepsilon)[v - u_\varepsilon] \ge 0 \qquad \forall v \in \mathcal{K}, \tag{2.13}$$

with

$$J'_\varepsilon(u)[\vartheta] = \int_\Omega (1-k)\vartheta \nabla S(u) \cdot \nabla p + \int_\Omega \vartheta S(u)^3 p + 2\alpha\varepsilon \int_\Omega \nabla u \cdot \nabla \vartheta + \frac{\alpha}{\varepsilon} \int_\Omega (1-2u)\vartheta; \tag{2.14}$$

where $\vartheta \in \mathcal{K} - u = \{v \text{ s.t. } u + v \in \mathcal{K}\}$ and p is the solution of the adjoint problem:

$$\int_\Omega a(u) \nabla p \cdot \nabla \psi + \int_\Omega 3b(u) S(u)^2 p \psi = \int_{\partial\Omega} (S(u) - y_{meas})\psi \qquad \forall \psi \in H^1(\Omega). \tag{2.15}$$

Proof. First of all we need to prove that S is Fréchet differentiable in $L^\infty(\Omega)$: in particular, we claim that for $\vartheta \in L^\infty(\Omega)\cap(\mathcal{K}-u)$ it holds that $S'(u)[\vartheta]=S_*$, where S_* is the solution in $H^1(\Omega)$ of

$$\int_\Omega a(u)\nabla S_*\nabla\varphi+\int_\Omega b(u)3S(u)^2S_*\varphi=\int_\Omega(1-k)\vartheta\nabla S\nabla\varphi+\int_\Omega \vartheta S(u)^3\varphi \quad \forall\varphi\in H^1(\Omega), \tag{2.16}$$

namely, that

$$\|S(u+\vartheta)-S(u)-S_*\|_{H^1(\Omega)}=o(\|\vartheta\|_{L^\infty(\Omega)}). \tag{2.17}$$

First we show that if $\vartheta\in L^\infty(\Omega)\cap(\mathcal{K}-u)$, then $\|S(u+\vartheta)-S(u)\|_{H^1(\Omega)}\le C\|\vartheta\|_{L^\infty(\Omega)}$. Indeed, the difference $w=S(u+\vartheta)-S(u)$ satisfies

$$\begin{aligned}\int_\Omega a(u+\vartheta)\nabla w\nabla\varphi+\int_\Omega b(u+\vartheta)qw\varphi=&-\int_\Omega(a(u+\vartheta)-a(u))\nabla S(u)\nabla\varphi\\&-\int_\Omega(b(u+\vartheta)-b(u))S(u)^3\varphi \qquad \forall\varphi\in H^1(\Omega),\end{aligned} \tag{2.18}$$

with $q=S(u+\vartheta)^2+S(u)S(u+\vartheta)+S(u)^2$. Substituting $a(u+\vartheta)-a(u)=-(1-k)\vartheta$ and $b(u+\vartheta)-b(u)=-\vartheta$, and taking $\varphi=w$ in (2.18), as in the proof of Proposition 2.5, we obtain

$$k\|\nabla w\|^2_{L^2}+\frac{3}{4}\int_\Omega b(u+\vartheta)S(u)^2w^2\le\|\vartheta\|_{L^\infty}\|\nabla S(u)\|_{L^2}\|\nabla w\|_{L^2}+\left\|S(u)^3\right\|_{L^2}\|w\|_{L^2}\|\vartheta\|_{L^\infty}$$

and again by Proposition 2.4

$$k\|\nabla w\|^2_{L^2}+\frac{3}{4}m^{2/3}\|w\|^2_{L^2(\Omega^{d_0})}\le\|\vartheta\|_{L^\infty}\|\nabla S(u)\|_{L^2}\|\nabla w\|_{L^2}+\|\vartheta\|_{L^\infty}\left\|S(u)^3\right\|_{L^2}\|w\|_{L^2}.$$

By (2.5) and the Sobolev inequality, eventually

$$\|w\|^2_{H^1(\Omega)}\le C\|S(u)\|_{H^1(\Omega)}\|w\|_{H^1(\Omega)}\|\vartheta\|_{L^\infty},$$

hence $\|S(u+\vartheta)-S(u)\|_{H^1(\Omega)}=O(\|\vartheta\|_{L^\infty(\Omega)})$.

Take now (2.18) and subtract (2.16). Define $r=S(u+\vartheta)-S(u)-S_*$: it holds that

$$\begin{aligned}\int_\Omega a(u)\nabla r\nabla\varphi+\int_\Omega b(u)3S(u)^2r\varphi=&\int_\Omega(a(u+\vartheta)-a(u))\nabla w\cdot\nabla\varphi\\&+\int_\Omega(b(u+\vartheta)q-3b(u)S(u)^2)w\varphi \qquad \forall\varphi\in H^1(\Omega).\end{aligned}$$

The second integral in the latter sum can be split as follows:

$$\int_\Omega(b(u+\vartheta)q-3b(u)S(u)^2)w\varphi=\int_\Omega(b(u+\vartheta)-b(u))qw\varphi+\int_\Omega(q-3S(u)^2)b(u)w\varphi,$$

and in particular $q-3S(u)^2=S(u+\vartheta)^2+S(u+\vartheta)S(u)-2S(u)^2=hw$, where $h=S(u+\vartheta)+2S(u)\in H^1(\Omega)$. Hence, choosing $\varphi=r$ and exploiting again Proposition 2.4, the Poincaré inequality in Lemma 2.1 and the Hölder inequality:

$$\begin{aligned}\frac{1}{C}\|r\|^2_{H^1}\le k\|\nabla r\|^2_{L^2}+m^{2/3}\|r\|_{L^2(\Omega^{d_0})}&\le(1-k)\|\vartheta\|_{L^\infty}\|\nabla w\|_{L^2}\|\nabla r\|_{L^2}\\&+\|\vartheta\|_{L^\infty}\|q\|_{L^4}\|w\|_{L^2}\|r\|_{L^4}+\|h\|_{L^4}\|w\|^2_{L^4}\|r\|_{L^4}\\&\le\Big((1-k)\|\vartheta\|_{L^\infty}\|w\|_{H^1}+\|q\|_{H^1}\|\vartheta\|_{L^\infty}\|w\|_{H^1}+\|h\|_{H^1}\|w\|^2_{H^1}\Big)\|r\|_{H^1}.\end{aligned}$$

It follows eventually that $\|r\|_{H^1(\Omega)} \leq C\|\vartheta\|_{L^\infty}^2 = o(\|\vartheta\|_{L^\infty})$, which guarantees that $S_* = S'(u)[\vartheta]$.

The last step is to provide an expression of the Fréchet derivative of J_ε. Exploiting the fact that S is differentiable, we can compute the expression of $J'_\varepsilon(u)$ through the *chain rule*:

$$J'_\varepsilon(u)[\vartheta] = \int_{\partial\Omega} (S(u)-y_0)S'(u)[\vartheta] + \alpha \int_\Omega \left(2\varepsilon \nabla u \nabla \vartheta + \frac{1}{\varepsilon}(1-2u)\vartheta \right). \tag{2.19}$$

Finally, thanks to the expression of the adjoint problem,

$$\int_{\partial\Omega} (S(u)-y_0)S'(u)[\vartheta] = \int_{\partial\Omega} (S(u)-y_0)S_* = \int_\Omega a(u)\nabla p \cdot \nabla S_* + \int_\Omega 3S(u)^2 p S_* =$$
$$\textit{(by definition of } S_*\textit{)} = \int_\Omega (1-k)\vartheta \nabla S(u)\cdot\nabla p + \int_\Omega \vartheta S(u)^3 p,$$

and hence:

$$J'_\varepsilon(u)[\vartheta] = \int_\Omega (1-k)\vartheta\nabla S(u)\cdot\nabla p + \int_\Omega \vartheta S(u)^3 p + \alpha \int_\Omega \left(2\varepsilon \nabla u \cdot \nabla\vartheta + \frac{1}{\varepsilon}(1-2u)\vartheta \right).$$

Finally, it is a standard argument that J_ε being a continuous and Fréchet differentiable functional on a convex subset $\mathcal{K}$ of the Banach space $H^1(\Omega)$, the optimality conditions for the optimization problem (2.12) are expressed by the variational inequality (2.13). □

3. Discretization and reconstruction algorithm

For a fixed $\varepsilon > 0$, we now introduce a finite element formulation of problem (2.12) in order to define a numerical reconstruction algorithm and compute an approximated solution of the inverse problem.

In what follows, we consider Ω to be polygonal, in order to avoid a discretization error involving the geometry of the domain. Let $\mathcal{T}_h$ be a shape regular triangulation of Ω and define $V_h \subset H^1(\Omega)$:

$$V_h = \{v_h \in C(\bar\Omega), v_h|_K \in \mathbb{P}_1(K)\ \forall K \in \mathcal{T}_h\}; \qquad \mathcal{K}_h = V_h \cap \mathcal{K}.$$

For every fixed $h > 0$, we define the solution map $S_h : \mathcal{K} \to V_h$, where $S_h(u)$ solves

$$\int_\Omega a(u)\nabla S_h(u)\nabla v_h + \int_\Omega b(u) S_h(u)^3 v_h = \int_\Omega f v_h \quad \forall v_h \in V_h.$$

3.1. Convergence analysis as $h \to 0$.

The present section is devoted to the numerical analysis of the discretized problem: the convergence of the approximated solution of the direct problem is studied, taking into account the difficulties implied by the nonlinear term. Moreover, the existence and convergence of minimizers of the discrete cost functional is analysed. The following result, which is preliminary for the proof of the convergence of the approximated solutions to the exact one, can be proved by resorting to the techniques of [18, Theorem 2.1].

LEMMA 3.1. *Let $f \in L^2(\Omega)$ satisfy Assumption (2.2); then, for every $u \in \mathcal{K}$, $S_h(u) \to S(u)$ strongly in $H^1(\Omega)$.*

Proof. As in the proof of Proposition 2.1, for a fixed $u \in \mathcal{K}$ we define the operator $T : H^1(\Omega) \to (H^1(\Omega))^*$ such that

$$\langle T(y), \varphi \rangle = \int_\Omega a(u)\nabla y \nabla\varphi + \int_\Omega b(u) y^3 \varphi;$$

then $y_h = S_h(u)$ and $y = S(u)$ are respectively the solutions of the equations

$$\langle T(y_h), \varphi_h\rangle = \int_\Omega f\varphi_h \qquad \forall \varphi_h \in V_h; \qquad \langle T(y), \varphi\rangle = \int_\Omega f\varphi \qquad \forall \varphi \in H^1(\Omega). \tag{3.1}$$

The ellipticity of the operator T follows from Lemma 2.1 and Proposition 2.4, indeed:

$$\begin{aligned}\langle T(y_h) - T(y), y_h - y\rangle &= \int_\Omega a(u)|\nabla(y_h - y)|^2 + \int_\Omega b(u)(y_h - y)^2(y_h^2 + y_h y + y^2)\\ &\geq k\|\nabla(y_h - y)\|^2_{L^2(\Omega)} + \frac{3}{4}m^{2/3}\|y_h - y\|^2_{L^2(\Omega^{d_0})} \geq C\|y_h - y\|^2_{H^1(\Omega)},\end{aligned}$$

where $C = C(k, m, \Omega, d_0)$ is independent of h. Consider now an arbitrary $w_h \in V_h$ and exploit the orthogonality $\langle T(y_h) - T(y), \varphi_h\rangle = 0\ \forall \varphi_h \in V_h$, which follows from (3.1).

$$\begin{aligned}C\|y_h - y\|^2_{H^1} &\leq \langle T(y_h) - T(y), y_h - y\rangle = \langle T(y_h) - T(y), w_h - y\rangle\\ &\leq K\|w_h - y\|_{H^1}\|y_h - y\|_{H^1},\end{aligned}$$

where K is the Lipschitz constant of T (see Proposition 2.1). We point out that, in view of Proposition 2.2, the constant K does not depend either on u or on h, but only on $\|f\|_{L^2(\Omega)}, \Omega, d_0, k$. Hence:

$$\|y_h - y\|_{H^1} \leq \frac{K}{C}\|w_h - y\|_{H^1},$$

and since the latter inequality holds for each $w_h \in H^1(\Omega)$, it holds:

$$\|y_h - y\|_{H^1(\Omega)} \leq \frac{K}{C}\inf_{w_h \in V_h}\|w_h - y\|_{H^1(\Omega)},$$

and the thesis follows from the interpolation estimates of $H^1(\Omega)$ functions in V_h. □

The convergence of the solution of the discrete direct problem to the continuous one is an immediate consequence of Lemma 3.1 and of the continuity of the map S_h in the space V_h, which can be assessed analogously to the proof of Proposition 2.5.

Proposition 3.1. *Let $\{h_k\}, \{u_k\}$ be two sequences such that $h_k \to 0$, $u_k \in \mathcal{K}_{h_k}$ and $u_k \xrightarrow{L^1} u \in \mathcal{K}$. Then $S_{h_k}(u_k) \xrightarrow{H^1} S(u)$.*

Define the discrete cost functional, $J_{\varepsilon,h} : \mathcal{K}_h \to \mathbb{R}$

$$J_{\varepsilon,h}(u_h) = \frac{1}{2}\|S_h(u_h) - y_{meas,h}\|^2_{L^2(\partial\Omega)} + \alpha\int_\Omega\left(\varepsilon|\nabla u_h|^2 + \frac{1}{\varepsilon}u_h(1 - u_h)\right), \tag{3.2}$$

with $y_{meas,h}$ being the $L^2(\Omega)$-projection of the boundary datum y_{meas} in the space of the traces of V_h functions. The existence of minimizers of the discrete functionals $J_{\varepsilon,h}$ is stated in the following proposition, together with an asymptotic analysis as $h \to 0$. Taking advantage of Proposition 3.1, the proof is analogous to the one of [20, Theorem 3.2].

Proposition 3.2. *For each $h > 0$, there exists $u_h \in \mathcal{K}_h$ such that $J_{\varepsilon,h}(u_h) = min_{v_h \in \mathcal{K}_h} J_{\varepsilon,h}(v_h)$. Every sequence $\{u_{h_k}\}$ s.t. $\lim_{k\to\infty} h_k = 0$ admits a subsequence that converges in $H^1(\Omega)$ to a minimum of the cost functional J_ε.*

The strategy we adopt in order to minimize the discrete cost functional $J_{\varepsilon,h}$ is to search for a function u_h satisfying discrete optimality conditions, which can be obtained as in Section 2.1:

$$J'_{\varepsilon,h}(u_h)[v_h - u_h] \geq 0 \quad \forall v_h \in \mathcal{K}_h \tag{3.3}$$

where for each $\theta_h \in \mathcal{K}_h - u_h := \{\theta_h = v_h - u_h;\ v_h \in \mathcal{K}_h\}$ it holds:

$$\begin{aligned} J'_{\varepsilon,h}(u_h)[\vartheta_h] = & \int_\Omega (1-k)\vartheta_h \nabla S_h(u_h)\cdot \nabla p_h + \int_\Omega \vartheta_h S_h(u_h)^3 p_h + 2\alpha\varepsilon \int_\Omega \nabla u_h \cdot \nabla \vartheta_h \\ & + \frac{\alpha}{\varepsilon}\int_\Omega (1-2u_h)\vartheta_h, \end{aligned} \tag{3.4}$$

where p_h is the solution in V_h of the adjoint problem (2.15) associated with u_h.

It is finally possible to demonstrate the convergence of critical points of the discrete functionals $J_{\varepsilon,h}$ (i.e., functions in $\mathcal{K}_h$ satisfying (3.3)) to a critical point of the continuous one, J_ε. The proof can be adapted from the one of [20, Theorem 3.2].

PROPOSITION 3.3. *Consider a sequence $\{h_k\}$ s.t. $h_k \to 0$ and for every k, denote as u_k, a solution of the discrete variational inequality* (3.3). *Then there exists a subsequence of $\{u_k\}$ that converges a.e and in $H^1(\Omega)$ to a solution u of the continuous variational inequality* (2.14)

3.2. Reconstruction algorithm: a parabolic obstacle problem approach. The necessary optimality conditions that have been stated in Proposition 2.10, together with the expression of the Fréchet derivative of the cost functional reported in (2.14), allow to define a parabolic obstacle problem, which consists of a very common strategy of searching for a solution of optimization problems in a phase-field approach. In this section we give a continuous formulation of the problem, and provide a formal proof of its desired properties. We then introduce a numerical discretization of the problem and rigorously prove the main convergence results.

The core of the proposed approach is to rely on a parabolic problem whose solution $u(\cdot,t)$ converges, as the fictitious time variable tends to $+\infty$, to an asymptotic state u_∞ satisfying the continuous optimality conditions (2.14). The problem can be formulated as follows, for a fixed $\varepsilon > 0$: let u be the solution of

$$\begin{cases} \displaystyle\int_\Omega \partial_t u(v-u) + J'_\varepsilon(u)[v-u] \geq 0 \qquad \forall v \in \mathcal{K}, \quad t \in (0,+\infty) \\ \qquad\qquad u(\cdot,0) = u_0 \in \mathcal{K}. \end{cases} \tag{3.5}$$

The theoretical analysis of the latter problem is beyond the purposes of this work, and would require to deal with the severe nonlinearity of the expression of $J'_\varepsilon(u)$; consequently, we provide a complete discretization of the parabolic obstacle problem and assess its convergence properties. This is performed by setting (3.5) in the discrete spaces $\mathcal{K}_h$ and V_h, and by considering a semi-implicit one-step scheme for the time updating, as in [20]: i.e., by treating explicitly the nonlinear terms and implicitly the linear ones. We obtain that the approximate solution $\{u_h^n\}_{n\in\mathbb{N}} \subset V_h$, $u_h^n \approx u(\cdot,t^n)$ is computed as:

$$\begin{cases} u_h^0 = u_0 \in \mathcal{K}_h \qquad \textit{(a prescribed initial datum)} \\ u_h^{n+1} \in \mathcal{K}_h : \int_\Omega (u_h^{n+1} - u_h^n)(v_h - u_h^{n+1}) + \tau_n \int_\Omega (1-k) \nabla S_h(u_h^n) \cdot \nabla p_h^n (v_h - u_h^{n+1}) \\ \qquad + \tau_n \int_\Omega S_h(u_h^n)^3 p_h^n (v_h - u_h^{n+1}) + 2\tau_n \alpha\varepsilon \int_\Omega \nabla u_h^{n+1} \cdot \nabla (v_h - u_h^{n+1}) \\ \qquad + \tau_n \alpha \frac{1}{\varepsilon} \int_\Omega (1-2u_h^n)(v_h - u_h^{n+1}) \geq 0 \quad \forall v_h \in \mathcal{K}_h,\ n = 0,1,\ldots \end{cases} \tag{3.6}$$

The following preliminary result is necessary for the proof of the convergence of the algorithm:

LEMMA 3.2. *For each $n > 0$, there exists a positive constant $\mathcal{B}_n = \mathcal{B}_n(\Omega, h, k, \|p_h^n\|_{H^1}, \|y_h^n\|_{H^1}, \|y_h^{n+1}\|_{H^1})$ such that, provided that $\tau_n \leq \mathcal{B}_n$, it holds that:*

$$\left\|u_h^{n+1} - u_h^n\right\|_{L^2}^2 + J_{\varepsilon,h}(u_h^{n+1}) \leq J_{\varepsilon,h}(u_h^n) \qquad n > 0. \tag{3.7}$$

Proof. In the expression of the discrete parabolic obstacle problem (3.6), consider $v_h = u_h^n$: via simple computation, we can point out that

$$\begin{aligned} &\frac{1}{\tau_n}\left\|u_h^{n+1} - u_h^n\right\|_{L^2}^2 + J(u_h^{n+1}) - J(u_h^n) + \alpha\varepsilon \left\|\nabla(u_h^{n+1} - u_h^n)\right\|_{L^2}^2 + \frac{\alpha}{\varepsilon}\left\|u_h^{n+1} - u_h^n\right\|_{L^2}^2 \\ &\leq \int_\Omega \left(a(u_h^{n+1}) - a(u_h^n)\right) \nabla y_h^n \nabla p_h^n + \int_\Omega \left(b(u_h^{n+1}) - b(u_h^n)\right) (y_h^n)^3 p_h^n \\ &\quad + \frac{1}{2}\left\|y_h^{n+1} - y_h^n\right\|_{L^2(\partial\Omega)}^2 + \int_{\partial\Omega} (y_h^{n+1} - y_h^n)(y_h^{n+1} - y_{meas,h}), \end{aligned}$$

where $y_h^n = S_h(u_h^n)$ and $y_h^{n+1} = S_h(u_h^{n+1})$. Moreover, by the expression of the adjoint problem,

$$RHS = \frac{1}{2}\left\|y_h^{n+1} - y_h^n\right\|_{L^2(\partial\Omega)}^2 + \textcircled{\scriptsize I} + \textcircled{\scriptsize II},$$

where

$$\begin{aligned} \textcircled{\scriptsize I} &= \int_\Omega \left(a(u_h^{n+1}) - a(u_h^n)\right) \nabla y_h^n \cdot \nabla p_h^n + \int_\Omega a(u_h^n) \nabla p_h^n \cdot \nabla (y_h^{n+1} - y_h^n) \\ &= \int_\Omega \left(a(u_h^n) - a(u_h^{n+1})\right) \nabla (y_h^{n+1} - y_h^n) \cdot \nabla p_h^n + \int_\Omega a(u_h^{n+1}) \nabla y_h^{n+1} \cdot \nabla p_h^n \\ &\quad - \int_\Omega a(u_h^n) \nabla y_h^n \cdot \nabla p_h^n; \end{aligned}$$

$$\begin{aligned} \textcircled{\scriptsize II} &= \int_\Omega \left(b(u_h^{n+1}) - b(u_h^n)\right) (y_h^n)^3 p_h^n + 3\int_\Omega b(u_h^n)(y_h^n)^2 p_h^n (y_h^{n+1} - y_h^n) = \\ &= \int_\Omega b(u_h^{n+1}) \left((y_h^n)^3 - (y_h^{n+1})^3\right) p_h^n + 3\int_\Omega b(u_h^n)(y_h^n)^2 p_h^n (y_h^{n+1} - y_h^n) \\ &\quad + \int_\Omega b(u_h^{n+1})(y_h^{n+1})^3 p_h^n - \int_\Omega b(u_h^n)(y_h^n)^3 p_h^n = \end{aligned}$$

$$\text{(by the expansion } (y_h^{n+1})^3 = \big(y_h^n + (y_h^{n+1} - y_h^n)\big)^3\text{)}$$
$$= 3\int_\Omega \big(b(u_h^n) - b(u_h^{n+1})\big)(y_h^n)^2 p_h^n (y_h^{n+1} - y_h^n) - 3\int_\Omega b(u_h^{n+1})(y_h^n)p_h^n(y_h^{n+1} - y_h^n)^2$$
$$- \int_\Omega b(u_h^{n+1}) p_h^n (y_h^{n+1} - y_h^n)^3 + \int_\Omega b(u_h^{n+1})(y_h^{n+1})^3 p_h^n - \int_\Omega b(u_h^n)(y_h^n)^3 p_h^n.$$

Collecting the terms and taking advantage of the expression of the direct problem, we conclude that

$$RHS = \frac{1}{2}\big\|y_h^{n+1} - y_h^n\big\|^2_{L^2(\partial\Omega)} + \int_\Omega \big(a(u_h^n) - a(u_h^{n+1})\big)\nabla(y_h^{n+1} - y_h^n)\cdot\nabla p_h^n$$
$$+ 3\int_\Omega \big(b(u_h^n) - b(u_h^{n+1})\big)(y_h^n)^2 p_h^n (y_h^{n+1} - y_h^n)$$
$$- 3\int_\Omega b(u_h^{n+1})(y_h^n)p_h^n(y_h^{n+1} - y_h^n)^2 - \int_\Omega b(u_h^{n+1})p_h^n(y_h^{n+1} - y_h^n)^3.$$

We now employ the Cauchy-Schwarz inequality and the regularity of the solutions of the discrete direct and adjoint problems (in particular the equivalence of the $W^{1,\infty}$ and H^1 norm in V_h: $\|u_h\|_{W^{1,\infty}} \le C_1\|u_h\|_{H^1}$, $C_1 = C_1(\Omega, h)$):

$$RHS \le C_2\big\|u_h^{n+1} - u_h^n\big\|_{L^2}\big\|y_h^{n+1} - y_h^n\big\|_{H^1} + C_3\big\|y_h^{n+1} - y_h^n\big\|^2_{H^1}$$

with $C_2 = (1-k)C_1\|p_h^n\|_{H^1} + C_1\|y_h^n\|_{H^1}\|p_h^n\|_{H^1}$ and $C_3 = 3C_1^2\|y_h^n\|_{H_1}\|p_h^n\|_{H_1} + C_1^3\|p_h^n\|_{H_1}(\|y_h^n\|_{H_1} + \big\|y_h^{n+1}\big\|_{H_1}) + \frac{1}{2}C_{tr}^2$, with C_{tr} being the constant of the trace inequality in $H^1(\Omega)$. Eventually, similar to the computation included in the proof of Proposition 2.10, one can assess that

$$\big\|y_h^{n+1} - y_h^n\big\|_{H^1} \le C_4\big\|u_h^{n+1} - u_h^n\big\|_{L^2},$$

with $C_4 = C_4(k, C_1, \|y_h^n\|_{H^1}, \Omega)$. Hence, we can conclude that there exists a positive constant $\mathcal{C}_n = C_2C_4 + C_3C_4^2$ such that

$$\frac{1}{\tau_n}\big\|u_h^{n+1} - u_h^n\big\|^2_{L^2} + J(u_h^{n+1}) - J(u_h^n) \le \mathcal{C}_n\big\|u_h^{n+1} - u_h^n\big\|^2_{L^2},$$

and choosing $\tau_n < \mathcal{B}_n := \frac{1}{1+\mathcal{C}_n}$ we can conclude the thesis. ∎

We are finally able to prove the following convergence result for the fully discretized parabolic obstacle problem:

PROPOSITION 3.4. *Consider a starting point $u_h^0 \in \mathcal{K}_h$. Then, there exists a collection of timesteps $\{\tau_n\}$ s.t. $0 < \gamma \le \tau_n \le \mathcal{B}_n$ $\forall n > 0$. Corresponding to $\{\tau_n\}$, the sequence $\{u_h^n\}$ generated by* (3.6) *has a converging subsequence (which we still denote with u_h^n) such that $u_h^n \xrightarrow{W^{1,\infty}} u_h \in V_h$, which satisfies the discrete optimality conditions* (3.3).

Proof. Consider a generic collection of timesteps $\tilde\tau_n$ satisfying $\tilde\tau_n \le \mathcal{B}_n$ $\forall n > 0$. Hence, by Lemma 3.2,

$$\sum_{n=0}^{\infty}\big\|u_h^{n+1} - u_h^n\big\|^2_{L^2} \le J_{\varepsilon,h}(u_h^0) \quad \text{and} \quad \sup_n J_{\varepsilon,h}(u_h^n) \le J_{\varepsilon,h}(u_h^0)$$

which implies that $\big\|u_h^{n+1} - u_h^n\big\|_{L^2} \to 0$ and hence u_h^n is bounded in $H^1(\Omega)$, and this implies that $\{y_h^n\}$ and $\{p_h^n\}$ are also bounded in $H^1(\Omega)$. According to the definition of the constants $\mathcal{C}_n$ and $\mathcal{B}_n$ reported in the proof of Lemma 3.2, this entails that there exists a constant $M>0$ such that $\mathcal{C}_n \leq M$ $\forall n>0$, and equivalently there exists a positive constant γ s.t. $\gamma \leq \mathcal{B}_n$. Hence, it is possible to choose, for each $n>0$, $\gamma \leq \tau_n \leq \mathcal{B}_n$. Eventually, we conclude that there exists $u_h \in \mathcal{K}_h$ such that, up to a subsequence, $u_h^n \to u_h$ a.e. and in $W^{1,\infty}(\Omega)$ (and $y_h^n \to y_h := S_h(u_h)$, $p_h^n \to p_h$ in H^1 and in $W^{1,\infty}$ as well, as in the discrete space V_h the L^∞ norm is equivalent to the $L^2(\Omega)$). We exploit the expression of the discrete parabolic obstacle problem (3.6) to show that

$$\int_\Omega (1-k)\nabla y_h^n \cdot \nabla p_h^n (v_h - u_h^{n+1}) + \int_\Omega (y_h^n)^3 p_h^n (v_h - u_h^{n+1}) + 2\alpha\varepsilon \int_\Omega \nabla u_h^{n+1} \cdot \nabla (v_h - u_h^{n+1})$$
$$+\alpha \frac{1}{\varepsilon} \int_\Omega (1-2u_h^n)(v_h - u_h^{n+1}) \geq -\frac{1}{\tau_n} \int_\Omega (u_h^{n+1} - u_h^n)(v_h - u_h^{n+1}) \quad \forall v_h \in \mathcal{K}_h,$$

and since -$\frac{1}{\tau_n} > -\frac{1}{\gamma}$ $\forall n$, when taking the limit as $n \to \infty$, the right-hand side converges to 0, which entails that u_h satisfies the discrete optimality conditions (3.3). □

In order to solve (3.6) we resort to the primal-dual active set method (PDAS), introduced in [11]. Thus, the final formulation of the reconstruction algorithm is the following:

Algorithm 1 Solution of the discrete parabolic obstacle problem

```
Set n = 0 and u_h^0 = u_0, the initial guess for the inclusion
while ||u_h^n - u_h^{n-1}||_{L^∞(Ω)} > tol_POP do
    solve the direct problem (2.3) with u = u_h^n
    solve the adjoint problem (2.15) with u = u_h^n
    compute u^{n+1} solving (3.6) via PDAS algorithm
    update n = n+1;
end while
return u_h^n
```

REMARK 3.1. It is a common practice to increase the performance of a reconstruction algorithm by taking advantage of multiple measurements. In this context, it is possible to suppose the knowledge of N_f different measurements of the electric potential on the boundary, $y_{meas,j}$ $j=1,\cdots,N_f$, associated with different source terms f_j. Therefore, instead of tackling the optimization of the mismatch functional J as in (2.10), it is possible to introduce the averaged cost functional $J^{TOT}(u) = \frac{1}{N_f}\sum_{j=1}^{N_f} J^j(u)$, where $J^j(u) = \frac{1}{2}\|S_j(u) - y_{meas,j}\|^2_{L^2(\partial\Omega)}$, with $S_j(u)$ being the solution of the direct problem (2.3) with source term $f = f_j$. The process of regularization, relaxation and computation of the optimality conditions is exactly the same as for J, and yields the same reconstruction algorithm as in Algorithm 1, where, at each timestep the solution of N^f direct and adjoint problem must be computed.

4. Numerical results

In this section we report various results obtained by applying Algorithm 1. In all the numerical experiments, we consider $\Omega = (-1,1)^2$ and we introduce a uniform and shape regular tessellation $\mathcal{T}_h$ of triangles. Due to the lack of experimental measures of the boundary datum y_{meas}, we make use of synthetic data, i.e., we simulate the direct problem via the finite element method, considering the presence of an ischemic region of prescribed geometry, and extract the value on the boundary of the domain. In order to avoid incurring an inverse crime (i.e. the performance of the reconstruction algorithm is improved by the fact that the exact data is synthetically generated with the same numerical scheme as that adopted in the algorithm), we introduce a more refined mesh $\mathcal{T}_h^{ex}$ on which the exact problem is solved, and interpolate the resulting datum y_{meas} on the mesh $\mathcal{T}_h$.

In the following test cases, we apply Algorithm 1 for the reconstructed inclusions of different geometries, in order to investigate the effectiveness of the introduced strategy. We use the same computational mesh $\mathcal{T}_h$ (mesh size $h=0.04$, nearly 6000 elements) for the numerical solution of the boundary value problems involved in the procedure, except for the generation of each synthetic data which is performed on different finer meshes $\mathcal{T}_h^{ex}$. According to Remark 3.1, we make use of $N_f=2$ different measurements, associated with the source terms $f_1(x,y)=x$ and $f_2(x,y)=y$. The main parameters for all the simulations lie in the ranges reported in Table 4.1. We make use of the same relationship between ε and τ as in [20]. The initial guess for each simulation is $u_0\equiv 0$.

α	ε	τ	tol_{POP}
$10^{-4}\div 10^{-3}$	$1/(8\pi)$	$(0.01\div 0.1)/\varepsilon$	10^{-4}

Table 4.1: *Range of the main parameters.*

In Figure 4.1 we report some of the iterations of Algorithm 1 for the reconstruction of a circular inclusion ($\alpha=0.0001$, $\tau=0.01/\varepsilon$). The boundary $\partial\omega$ is marked with a black line, which is superimposed on the contour plot of the approximation of the indicator function u_h^n at different timesteps n. The algorithm converged after $N_{tot}=568$ iterations, corresponding to a final (fictitious) time $T_{tot}=1427.54$. In Figure 4.2 we investigate the effectiveness of the algorithm to reconstruct inclusions of rather complicated geometry. For each test case, we show the contour plot of the final iteration of the reconstruction (the total number of iterations N and the final time T are reported in the caption), and the boundary of the exact inclusion is overlaid in a black line. Moreover, each result is equipped with the graphic (in semilogarithmic scale) of the evolution of the cost functional J_ε, split into the components $J_{PDE}(u)=\frac{1}{2}\|S(u)-y_{meas}\|^2_{L^2(\partial\Omega)}$ and $J_{regularization}(u)=\alpha\varepsilon\|\nabla u\|^2_{L^2(\Omega)}+\frac{\alpha}{\varepsilon}\int_\Omega u(1-u)$. The reported results consist of approximations of minimizers of J_ε in $\mathcal{K}$: they are smooth functions and range between 0 and 1. They show large regions in which they attain the limit values 0 and 1, and a region

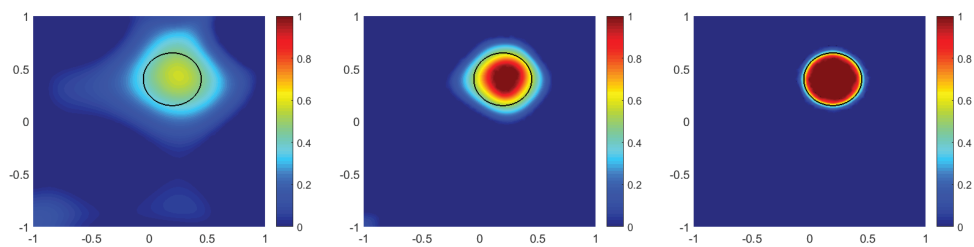

(a) $n=30$ (b) $n=90$ (c) $n=568$

Fig. 4.1: *Reconstruction of a circular inclusion: successive iterations.*

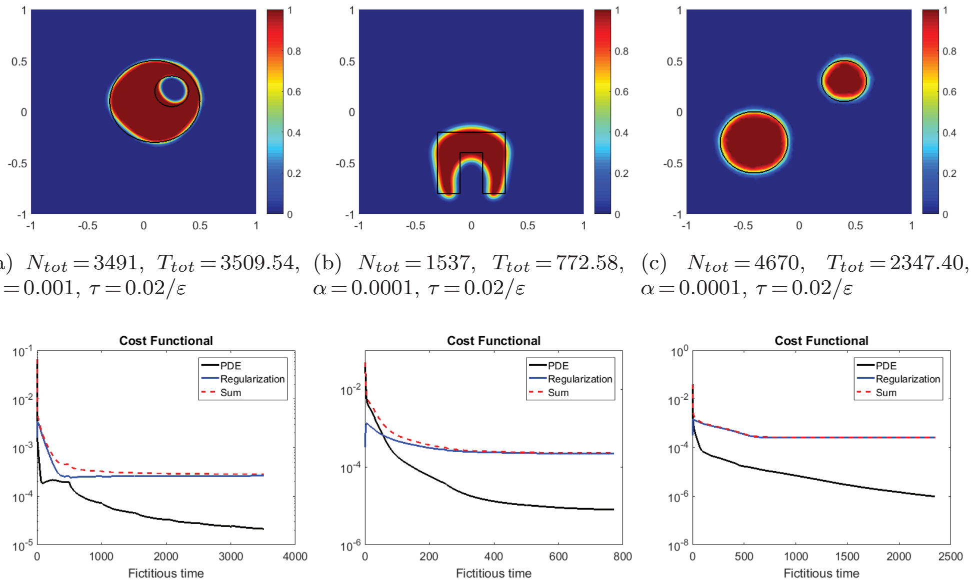

(a) $N_{tot}=3491$, $T_{tot}=3509.54$, $\alpha=0.001$, $\tau=0.02/\varepsilon$
(b) $N_{tot}=1537$, $T_{tot}=772.58$, $\alpha=0.0001$, $\tau=0.02/\varepsilon$
(c) $N_{tot}=4670$, $T_{tot}=2347.40$, $\alpha=0.0001$, $\tau=0.02/\varepsilon$
(d) Ellipse: evolution of J_ε
(e) Rectangle: evolution of J_ε
(f) Two circles: evolution of J_ε

Fig. 4.2: *Reconstruction of various inclusions.*

of *diffuse interface* between them, whose thickness is about $\varepsilon/2$. As Figures 4.1 and 4.2 show, the algorithm is able to reconstruct inclusions of rather complicated geometry. The identification of a smooth inclusion is performed with higher precision, whereas it seems that the accuracy is low in presence of sharp corners. We point out that we do not need to have any *a priori* knowledge on the topology of the inclusion ω, i.e., the number of connected components is correctly identified.

We now assess that the final result of the reconstruction is independent of the initial guess imposed as a starting point of the parabolic obstacle problem. In Figure 4.3 we compare the behaviour of the algorithm applied to the reconstruction of a circular inclusion (the same as in Figure 4.1), where we impose a different initial datum with respect to the constant zero function. In the first experiment, we start from an initial datum which is the indicator function of an arbitrarily chosen region. In the second one, we impose as a starting point the indicator function of a sublevel of the *topological gradient* of the cost functional J. As investigated in [10], the topological gradient is a powerful tool for the detection of small-size inclusions, which yield a small perturbation in the cost functional with respect to the background (unperturbed) case. The position of a small inclusion is easily identified by searching for the point where the topological gradient of J attains its (negative) minimum. As the information given by the topological gradient G has shown to be useful even in the case of large-size inclusions (see, e.g., [7, 14]), we take advantage of it by computing G (see Theorem 3.1 in [10]), setting a threshold G_{thr} and defining $u_0=\chi_{\{G\leq G_{thr}\}}$. The results reported in Figure 4.3 show the starting point of the algorithm, an intermediate iteration and the final reconstruction. In both cases we set $\alpha=0.001$, $\varepsilon=1/(8\pi)$ and $\tau=0.1/\varepsilon$. We underline that the result in each case is similar to the one depicted in Figure 4.1, but through the second strategy it was possible to perform a smaller number of iterations.

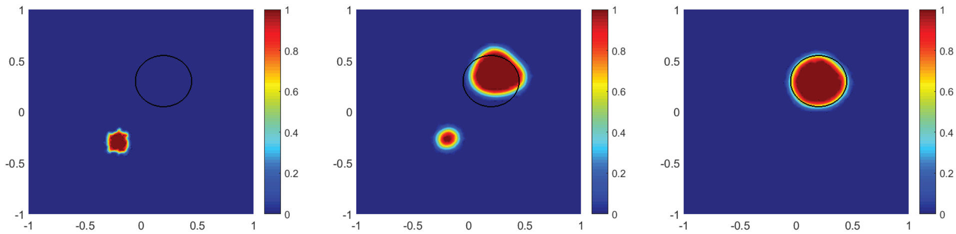

(a) Initial guess: arbitrary (b) Intermediate: $n = 60$ (c) Final: $N_{tot} = 661$, $T_{tot} = 1661.27$

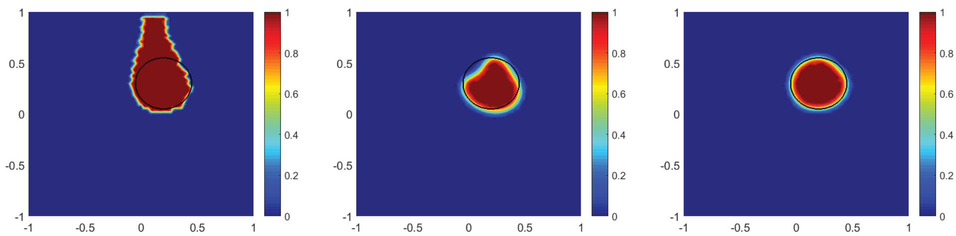

(d) Initial guess: topological (e) Intermediate: $n = 50$ (f) Final: $N_{tot} = 489$, $T_{tot} = 1228.99$

Fig. 4.3: *Reconstruction of a circular inclusion with different initial conditions.*

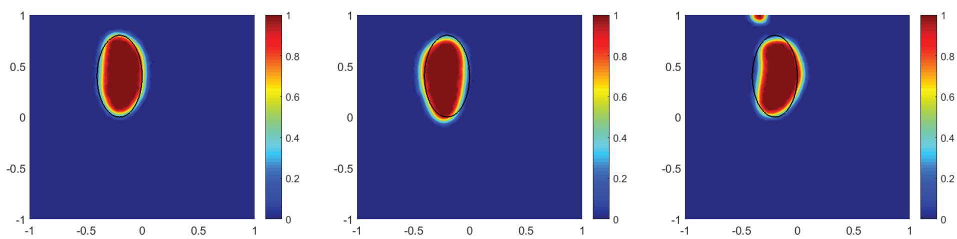

(a) $p = 0.01$; $N_{tot} = 430$ (b) $p = 0.05$; $N_{tot} = 503$ (c) $p = 0.1$; $N_{tot} = 1120$

Fig. 4.4: *Reconstruction of an elliptical inclusion with noisy measurements.*

We finally verify the stability result obtained in Proposition 2.7, by testing the reconstruction algorithm when the measured boundary data are perturbed by a small amount of noise. In particular, we consider $y_p = y_{meas} + p\eta$, η being a Gaussian random variable with null mean and standard deviation equal to $\max_\Omega y_{meas} - \min_\Omega y_{meas}$ and $p \in [0,1]$ being the noise level. In Figure 4.4 we report the final results of the reconstruction algorithm when applied to the boundary measurements related to an elliptical inclusion perturbed with different noise levels. For each simulation, we fix $\alpha = 0.001$ and $\varepsilon = \frac{1}{8\pi}$.

In Figure 4.5, we investigate the effect of the regularization parameter α on the reconstruction from noisy data, fixing $p = 0.1$. We observe that a higher value of α

may help in filtering the information coming from the noise, avoiding spoiling of the reconstruction, although it might result in an overall loss of precision.

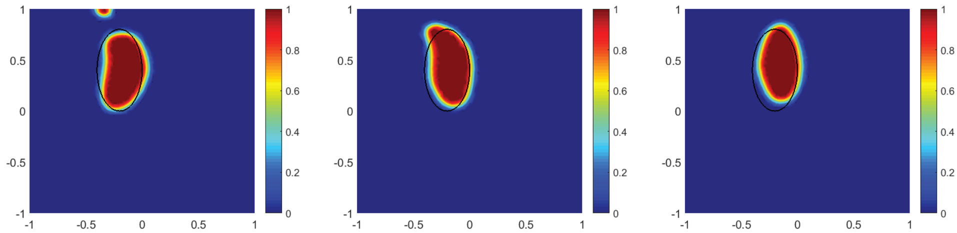

(a) $\alpha = 0.001$; $N_{tot} = 1120$ (b) $\alpha = 0.003$; $N_{tot} = 751$ (c) $\alpha = 0.01$; $N_{tot} = 462$

Fig. 4.5: *Reconstruction of an elliptical inclusion with noisy measurements.*

5. Comparison with the shape derivative approach

In the previous sections, we have analyzed in detail the phase-field relaxation of the minimization problem expressed in (2.11). We now aim at describing the relationship between this method and a shape derivative based approach, which consists of updating the shape of the inclusion to be reconstructed by perturbing its boundary along the directions of the vector field which causes the greatest descent of the cost functional. Such a direction can be deduced by computing the shape derivative of the functional itself. In this section, we first theoretically investigate the relationship between the shape derivative of the cost functional J_{reg} and the Fréchet derivative of J_ε and then report a comparison between the numerical results of the two algorithms in a set of benchmark cases.

5.1. Sharp interface limit of the optimality conditions. In order to study the relationship between the optimality conditions in the phase-field approach and the ones derived in the sharp case, we follow an analogous approach as in [12]. First of all, in Proposition 5.1 we introduce the necessary optimality condition for the sharp problem (2.11), taking advantage of the computation of the material derivative of the cost functional. We then define in Proposition 5.3 similar optimality conditions for the relaxed problem (2.12), which are related but not equivalent to the ones stated in (2.13) and (2.14) through the Fréchet derivative. In Proposition 5.4 we finally assess the convergence of the phase-field optimality condition to the sharp one when $\varepsilon \to 0$.

For the sake of simplicity, in this section we will refer to J_{reg} as J. Consider the minimization problem (as in (2.11)):

$$\underset{u \in X_{0,1}}{\arg\min}\, J(u); \quad J(u) = \frac{1}{2}\|S(u) - y_{meas}\|^2_{L^2(\partial\Omega)} + \alpha TV(u). \tag{5.1}$$

Since $u \in X_{0,1}$ implies that $u = \chi_\omega$, with ω being a finite-perimeter subset of Ω, we can perturb u by means of a vector field $\phi_t : \Omega \to \mathbb{R}^2$, $\phi_t(x) = x + tV(x)$, being

$$V \in C^1(\Omega) \text{ s.t. } V(x) = 0 \text{ in } \Omega^{d_0} = \{x \in \Omega \; s.t. \; dist(x, \partial\Omega) \leq d_0\}. \tag{5.2}$$

Consider the family of functions $\{u_t\}$: $u_t = u \circ \phi_t^{-1}$: we can compute the shape derivative of the functional J in u along the direction V (see [21]) as

$$DJ(u)[V] := \lim_{t \to 0} \frac{J(u_t) - J(u)}{t}, \tag{5.3}$$

where $J(u_t)$ is the cost functional evaluated in the deformed domain $\Omega_t = \phi_t(\Omega)$ but, according to (5.2), Ω_t and Ω are the same set, thus we do not adopt a different notation. We prove the following result:

PROPOSITION 5.1. *If u is a solution of* (5.1) *and $f \in L^2(\Omega)$ satisfies Assumption* (2.2), *then*

$$DJ(u)[V] = 0 \qquad \text{for all the smooth vector fields } V. \tag{5.4}$$

The shape derivative is given by:

$$DJ(u)[V] = \int_{\partial\Omega} (S(u) - y_{meas})\dot{S}(u)[V] + \int_{\Omega} (divV - DV\nu \cdot \nu) d|Du|, \tag{5.5}$$

where $d|Du| = \delta_{\partial\omega} dx$, ν is the generalized unit normal vector (see [27]) and $\dot{S}(u)[V] =: \dot{S}$, the material derivative of the solution map, solves

$$\int_\Omega a(u)\nabla\dot{S}\cdot\nabla v + \int_\Omega b(u)3S(u)^2\dot{S}v = -\int_\Omega a(u)\mathcal{A}\nabla S(u)\cdot\nabla v - \int_\Omega b(u)S(u)^3 v divV + \int_\Omega div(fV)v \qquad \forall v \in H^1(\Omega), \tag{5.6}$$

where $\mathcal{A} = divV - (DV + DV^T)$.

Proof. We start by deriving the formula of the material derivative of the solution map. Define $S_0 = S(u)$ and $S_t : \Omega \to \mathbb{R}$, $S_t = S(u_t) \circ \phi_t$. Then, applying the change of variables induced by the map ϕ_t, it holds that

$$\int_\Omega a(u)A(t)\nabla S_t \cdot \nabla v + \int_\Omega b(u)S_t^3 v|detD\phi_t| = \int_\Omega (f \cdot \phi_t)v|detD\phi_t| \qquad \forall v \in H^1(\Omega), \tag{5.7}$$

where $A(t) = D\phi_t^{-T} D\phi_t^{-1}|detD\phi_t|$. By computation,

$$\frac{d}{dt}A(t) = \mathcal{A} = (divV)I - (DV^t + DV) \qquad \text{and} \qquad \frac{d}{dt}|detD\phi_t| = divV.$$

Subtract (2.3) from (5.7) and divide by t: then $w_t = \frac{S_t - S_0}{t}$ is the solution of

$$\begin{aligned}\int_\Omega a(u)A(t)\nabla w_t \cdot \nabla v + \int_\Omega b(u)q_t w_t v|det(D\phi_t)| = -\int_\Omega a(u)\frac{A(t)-I}{t}\nabla S_0 \cdot \nabla v \\ -\int_\Omega \frac{|det(D\phi_t)|-1}{t} b(u)S_0^3 v + \int_\Omega \frac{1}{t}(f \circ \phi_t)v|det(D\phi_t)| - \int_\Omega \frac{1}{t}fv\end{aligned} \tag{5.8}$$

$\forall v \in H^1(\Omega)$, where the norm of the right-hand side in the dual space of $H^1(\Omega)$ is bounded by

$$\begin{aligned}\left\|\frac{A-I}{t}\right\|_{L^\infty(\Omega)} \|S_0\|_{H^1(\Omega)} + \left\|\frac{|det(D\phi_t)|-1}{t}\right\|_{L^\infty(\Omega)} \|S_0\|_{H^1(\Omega)} \\ + \left\|\frac{|det(D\phi_t)|-1}{t}\right\|_{L^\infty(\Omega)} \|f\|_{L^2(\Omega)} + C(\|V\|_{C(\Omega)})\|f\|_{H^1(\Omega)} \le C_F,\end{aligned}$$

with C_F independent of t. Moreover, the matrix $A(t)$ is symmetric positive definite: $(A(t)y)\cdot y \ge \frac{1}{2}\|y\|^2$ $\forall y \in \mathbb{R}^2, \forall t$. Together with the property that $q_t = u_t^2 + u_t u + u^2 \ge \frac{3}{4}u^2$, and thanks to Proposition 2.4 and to the Poincaré inequality in Lemma 2.1,

$$\|w_t\|_{H^1}^2 \le C\left(k\|\nabla w_t\|_{L^2}^2 + \frac{3}{4}m^{2/3}\|w_t\|_{L^2(\Omega^{d_0})}^2\right) \le C_F\|w_t\|_{H^1}.$$

Thus, $\|w_t\|_{H^1}$ is bounded independently of t, from which it follows that $\|S_t - S_0\|_{H^1(\Omega)} \leq Ct$ and that every sequence $\{w_n\} = \{w_{t_n},\ t_n \to 0\}$ is bounded in $H^1(\Omega)$, thus $w_t \xrightarrow{H^1} w \in H^1(\Omega)$. We aim at proving that w is also the limit of w_t in the strong convergence, which entails that

$$\dot{S}(u)[V] := \lim_{t\to 0} \frac{S_t - S_0}{t} = w.$$

First of all, we show that w is the solution of problem (5.6). It follows from (5.8), since $q_t w_t = \frac{1}{t}(S_t^3 - S_0^3) = \frac{1}{t}((S_0 + tw_t)^3 - S_0^3) = 3S_0^2 w_t + 3tS_0 w_t^2 + t^2 w_t^3$, that

$$\begin{aligned}
&\int_\Omega a(u)A(t)\nabla w_t \cdot \nabla v + \int_\Omega b(u)3S_0^2 w_t v |detD\phi_t| = -\int_\Omega a(u)\frac{A(t)-I}{t}\nabla S_0 \cdot \nabla v \\
&\quad - \int_\Omega \frac{|detD\phi_t| - 1}{t} b(u)S_0^3 v - \int_\Omega b(u)3tS_0 w_t^2 v|detD\phi_t| - \int_\Omega b(u)t^2 w_t^3 v |detD\phi_t| \\
&\quad + \int_\Omega (f\circ\phi_t)\frac{|detD\phi_t| - 1}{t} v - \int_\Omega \frac{(f\circ\phi_t) - f}{t} v \qquad \forall v \in H^1(\Omega).
\end{aligned} \tag{5.9}$$

Taking the limit as $t \to 0$ and by the weak convergence of w_t in H^1, we recover the same expression as in (5.6). One may eventually show that $w_t \xrightarrow{H^1} w$. In order to do this we start by proving that

$$\int_\Omega a(u)A(t)|\nabla w_t|^2 + \int_\Omega b(u)|detD\phi_t| 3S_0^2 w_t^2 \to \int_\Omega a(u)|\nabla w|^2 + \int_\Omega b(u)3S_0^2 w^2. \tag{5.10}$$

Indeed, take (5.9) and substitute $v = w_t$: using the weak convergence of w_t in the right-hand side, we obtain that

$$\begin{aligned}
\int_\Omega a(u)A(t)|\nabla w_t|^2 + \int_\Omega b(u)|detD\phi_t| 3S_0^2 w_t^2 &\to -\int_\Omega a(u)\mathcal{A}\nabla S_0 \cdot \nabla w - \int_\Omega divV\ b(u)S_0^3 w \\
&+ \int_\Omega fw\ divV - \int_\Omega \nabla f \cdot Vw \overset{(5.6)}{=} \int_\Omega a(u)|\nabla w|^2 + \int_\Omega b(u)3S_0^2 w^2.
\end{aligned}$$

We then compute:

$$\begin{aligned}
&\int_\Omega a(u)A(t)|\nabla(w_t - w)|^2 + \int_\Omega b(u)3S_0^2(w_t - w)^2|detD\phi_t| \\
&= \int_\Omega a(u)A(t)|\nabla w_t|^2 + \int_\Omega a(u)A(t)|\nabla w|^2 - 2\int_\Omega a(u)A(t)\nabla w_t \cdot \nabla w \\
&\quad + \int_\Omega b(u)3S_0^2 w_t^2 |detD\phi_t| + \int_\Omega b(u)3S_0^2 w^2|detD\phi_t| - 2\int_\Omega b(u)3S_0^2 w_t w |detD\phi_t|.
\end{aligned} \tag{5.11}$$

Using (5.10), the convergence of A to I and of $|detD\phi_t|$ to 1, and the fact that $w_t \xrightarrow{H^1} w$, we derive that

$$\int_\Omega a(u)|\nabla(w_t - w)|^2 + \int_\Omega b(u)3S_0^2(w_t - w)^2 \to 0$$

A combination of the Proposition 2.4 and of the Poincaré inequality in Lemma 2.1 allows to also conclude that $\|w_t - w\|_{H^1} \to 0$.

We now prove the necessary optimality conditions for the optimization problem (5.1). The derivative of the quadratic part of the cost functional J can be easily computed by means of the material derivative of the solution map:

$$\begin{aligned}
&\lim_{t\to 0}\frac{1}{2}\int_{\partial\Omega}\frac{(S(u_t)-y_{meas})^2|det(D\phi_t)|-(S_0-y_{meas})^2}{t} \qquad \textit{(since } S(u_t)=S_t \textit{ on } \partial\Omega\textit{)}\\
&=\lim_{t\to 0}\frac{1}{2}\int_{\partial\Omega}(S_t-y_{meas})^2\frac{|det(D\phi_t)|-1}{t}+\lim_{t\to 0}\frac{1}{2}\int_{\partial\Omega}\frac{(S_t-y_{meas})^2-(S_0-y_{meas})^2}{t}\\
&=\frac{1}{2}\int_{\partial\Omega}(S_0-y_{meas})^2 divV+\int_{\partial\Omega}\dot{S}(u)[V](S_0-y_{meas}),
\end{aligned}\tag{5.12}$$

and the first integral in the latter expression vanishes since $V=0$ on Ω_{d_0}. On the other hand, using Lemma 10.1 of [27] and the remark 10.2, we recover the expression for the derivative of the total variation of u, which is the same as in (5.5). ∎

The optimality conditions reported in (5.4) are, to the best of our knowledge, the most general result which can be obtained in this case, i.e. by simply assuming that $u=\chi_\omega$ and ω is a set of finite perimeter. We point out that, assuming more *a priori* information on u, it is possible to recover from (5.5) the expression of the *shape derivative* of the cost functional J. The following proposition can be rigorously proved by means of an argument similar to the one used in [2], except for the derivative of the perimeter penalization, which can be found in Section 9.4.3 in [21].

PROPOSITION 5.2. *Suppose that $\omega\subset\Omega$ is open, connected, well separated from the boundary $\partial\Omega$ and regular (at least of class C^2), and $u=\chi_\omega$. Then, the expression of the shape derivative of the cost functional J along a smooth vector field V is:*

$$DJ(u)[V]=\int_{\partial\omega}\left[(1-k)\left(\nabla_\tau S(u)\cdot\nabla_\tau w+\frac{1}{k}\nabla_\nu S(u)^e\cdot\nabla_\nu w^e\right)+S(u)^3w+\mathcal{H}\right]V\cdot\nu,\tag{5.13}$$

where w is the solution of the adjoint problem (see (2.15)). The gradients $\nabla S(u)$ and ∇w are decomposed in the normal and tangential components with respect to the boundary $\partial\omega$, and due to the transmission condition of the direct problem their normal components are discontinuos across $\partial\omega$: the value assumed in $\Omega\setminus\omega$ is marked as $\nabla_\nu S(u)^e$. The term $\mathcal{H}$ is instead the curvature of the boundary.

For the sake of completeness, we point out that the latter result can be easily generalized to the case in which ω is the union of N_c disjoint, well-separated components, each of them satisfying the expressed hypotheses. Thanks to the results recently obtained in [9], we expect formula (5.13) to also be valid under milder assumptions, in particular for polygons.

We aim at demonstrating that the expression of the shape derivative reported in (5.4) is the limit, as $\varepsilon\to 0$, of the shape derivative of the relaxed cost functional J_ε (defined as in (5.3), replacing u by u_ε and J by J_ε). In order to accomplish this result, we need to introduce necessary optimality conditions for the relaxed problem (2.12), which are different from the ones reported in Proposition 2.10 and can be derived by the same technique as in Proposition 5.1 as shown in the following result.

PROPOSITION 5.3. *If u_ε is a solution of (2.12), then*

$$DJ_\varepsilon(u_\varepsilon)[V]=0 \qquad \textit{for all the smooth vector fields } V,\tag{5.14}$$

The expression of the derivative is given by:

$$DJ_\varepsilon(u_\varepsilon)[V] = \int_{\partial\Omega} (S(u_\varepsilon) - y_{meas})\dot{S}(u_\varepsilon)[V] + \alpha\varepsilon \int_\Omega |\nabla u_\varepsilon|^2 divV$$
$$-2\alpha\varepsilon \int_\Omega DV \nabla u_\varepsilon \cdot \nabla u_\varepsilon + \frac{\alpha}{\varepsilon}\int_\Omega u_\varepsilon(1-u_\varepsilon) divV \tag{5.15}$$

where $\dot{S}(u_\varepsilon)[V]$ *solves the same problem as in* (5.6), *replacing* u *with* u_ε.

Proof. The same strategy as in the proof of Proposition 5.1 can be adapted to compute $\dot{S}(u_\varepsilon)[V]$ and the derivative of the first term of the cost functional. We now derive with the same computational rules the relaxed penalization term. Recall

$$F_\varepsilon(u_\varepsilon) = \alpha\varepsilon \int_\Omega |\nabla u_\varepsilon|^2 + \frac{\alpha}{\varepsilon}\int_\Omega \psi(u_\varepsilon),$$

being $\psi : \mathbb{R} \to \mathbb{R}$, $\psi(x) = x(1-x)$. After the deformation from u_ε to $u_\varepsilon \circ \phi_t^{-1}$ and applying the change of variables induced by ϕ_t,

$$F_\varepsilon(u_\varepsilon \circ \phi_t^{-1}) = \alpha\varepsilon \int_\Omega A(t)\nabla u_\varepsilon \cdot \nabla u_\varepsilon + \frac{\alpha}{\varepsilon}\int_\Omega \psi \circ u_\varepsilon \circ \phi_t^{-1}.$$

Hence,

$$\dot{F}_\varepsilon(u_\varepsilon)[V] = \lim_{t\to 0} \frac{F_\varepsilon(u_\varepsilon \circ \phi_t^{-1}) - F_\varepsilon(u_\varepsilon)}{t} = \alpha\varepsilon \int_\Omega \mathcal{A}\nabla u_\varepsilon \cdot \nabla u_\varepsilon + \alpha\varepsilon \frac{\alpha}{\varepsilon}\int_\Omega \psi(u_\varepsilon) divV$$
$$= \alpha\varepsilon \int_\Omega |\nabla u_\varepsilon|^2 divV - \alpha\varepsilon \int_\Omega (DV + DV^T)\nabla u_\varepsilon \cdot \nabla u_\varepsilon + \frac{\alpha}{\varepsilon}\int_\Omega u_\varepsilon(1-u_\varepsilon) divV,$$

which is the same expression as in (5.15), since $DV^T \nabla v \cdot \nabla v = DV \nabla v \cdot \nabla v$. ∎

We point out that the optimality conditions deduced in the latter proposition are not equivalent to the ones expressed in Proposition 2.10 via the Fréchet derivative of J_ε. Nevertheless, if u_ε satisfies (2.13)-(2.14), then it also satisfies (5.14) (it is sufficient to consider in (2.13) $v = u_\varepsilon \circ \phi_t^{-1}$, which belongs to $\mathcal{K}$ thanks to the regularity of V), whereas the contrary is not valid in general. In particular, due to the regularity of the perturbation fields V, the optimality conditions (5.14) do not take into account possible topological changes of the inclusion: for example, the number of connected components of ω cannot change. We remark that this holds also for the optimality conditions (5.4) for the sharp problem, and consists of a limitation for the effectiveness of the reconstruction via a shape derivative approach: the initial guess of the reconstruction algorithm and the exact inclusion must be diffeomorphic.

We are now able to show the sharp interface limit of the expression of the shape derivative of the relaxed cost functional J_ε as $\varepsilon \to 0$, which is done in the following proposition.

Proposition 5.4. *Consider a family* $\bar{u}_\varepsilon$ *s.t.* $\bar{u}_\varepsilon \in \mathcal{K}$ $\forall \varepsilon > 0$ *and* $\bar{u}_\varepsilon \xrightarrow{L^1} \bar{u} \in BV(\Omega)$ *as* $\varepsilon \to 0$. *Then,*

$$DJ_\varepsilon(\bar{u}_\varepsilon)[V] \to DJ(\bar{u})[V] \qquad \textit{for every smooth vector field } V.$$

Proof. We follow a similar argument as in the proof of [12, Theorem 21]. Thanks to Proposition 2.5, $\bar{u_\varepsilon} \xrightarrow{L^1} \bar{u} \Rightarrow S(\bar{u_\varepsilon}) \xrightarrow{H^1} S(\bar{u})$. Also $\dot{S}(\bar{u_\varepsilon})[V] \xrightarrow{H^1} \dot{S}(\bar{u})[V]$: the proof is done by subtracting the equations of $\dot{S}(\bar{u_\varepsilon})[V]$ and $\dot{S}(\bar{u})[V]$ and verifying that the norm of their difference is controlled by the norm of $S(\bar{u_\varepsilon})-S(\bar{u})$ in $H^1(\Omega)$. Thanks to these results, surely

$$\int_\Omega (S(u_\varepsilon)-y_{meas})\dot{S}(\bar{u_\varepsilon})[V] \to \int_\Omega (S(u)-y_{meas})\dot{S}(\bar{u})[V].$$

Eventually, the convergence

$$\alpha\varepsilon\int_\Omega |\nabla\bar{u_\varepsilon}|^2 divV - 2\alpha\varepsilon\int_\Omega DV\nabla\bar{u_\varepsilon}\cdot\nabla\bar{u_\varepsilon} + \frac{\alpha}{\varepsilon}\int_\Omega \bar{u_\varepsilon}(1-\bar{u_\varepsilon})divV \to \int_\Omega (divV - DV\nu\cdot\nu)d|D\bar{u}|$$

is proved in [25], Theorem 4.2 (see also annotations in [12], proof of Theorem 21). □

In particular, we point out that this implies, together with Proposition 2.9, that the expression of the optimality condition for the phase-field problem converges, as $\varepsilon\to 0$, to the one for the sharp case.

5.2. Comparison with the shape derivative algorithm. In this section, we report some results of the application of the algorithm based on the shape derivative. In the implementation, we take advantage of the finite element method to solve the direct and adjoint problems and compute the shape gradient as in (5.13). We consider an initial guess for the inclusion (in all the simulations reported, the initial guess is a disc centered in the origin with radius 0.02) and discretize its boundary with a finite number of points, which always coincide with vertices of the numerical mesh. We iteratively perturb the inclusion by moving the boundary with a normal vector field V which is the projection in the finite element space of the shape gradient reported in (5.13) (see e.g. [22] for more details). After the descent direction is determined, a backtracking scheme is implemented (see [36]), in order to guarantee the decrease of the cost functional J at each iteration. As in the case of Algorithm 1, we start from the initial guess $u^0\equiv 0$ and take advantage of $N_f=2$ measurements, associated with the same source terms. The main parameters of this set of simulations are reported in Table 5.1.

α	$maxstep$	tol
10^{-3}	10	10^{-6}

Table 5.1: *Values of the main parameters.*

In Figure 5.1 we report the results of the reconstruction with the shape gradient algorithm compared to the ones of the parabolic obstacle problem (with $\varepsilon=\frac{1}{16\pi}$ and with mesh adaptation). Each result is endowed with a plot of the evolution of the cost functional throughout time (in particular, of $J_{PDE}(u)=\frac{1}{2}\|S(u)-y_{meas}\|_{L^2(\partial\Omega)}$).

The reconstruction achieved by the shape gradient algorithm is qualitatively as accurate as the phase-field one. The first method is less expensive in terms of number of iterations. Nevertheless, it requires *a priori* knowledge about the topology of the unknown inclusion.

Acknowledgments. The authors are grateful to the reviewers for their careful reading and insightful comments on the paper. E. Beretta and M. Verani thank the New York University in Abu Dhabi for its kind hospitality that permitted a further development of the present research. We acknowledge the use of the MATLAB library redbKIT [35] for the numerical simulations presented in this work.

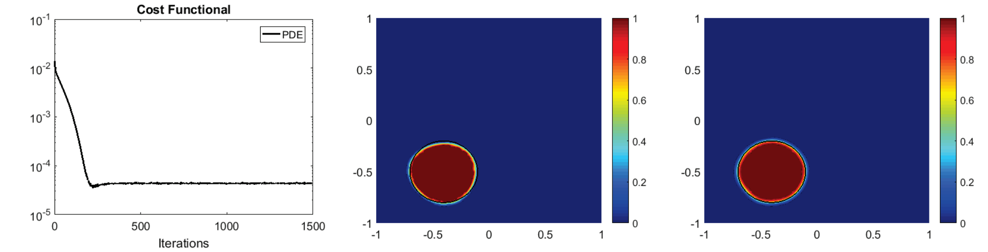

(a) Shape gradient, evolution of the cost functional (b) Shape gradient, $N_{tot} = 1494$ (c) Phase field, $\varepsilon = \frac{1}{16\pi}$, $N_{tot} = 1869$

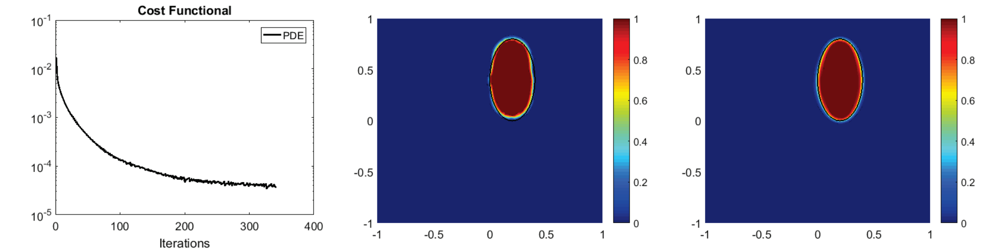

(d) Shape gradient, evolution of the cost functional (e) Shape gradient, $N_{tot} = 301$ (f) Phase field, $\varepsilon = \frac{1}{16\pi}$, $N_{tot} = 1503$

Fig. 5.1: *Shape gradient algorithm: result comparison.*

REFERENCES

[1] L. Afraites, M. Dambrine, and D. Kateb, *Conformal mappings and shape derivatives for the transmission problem with a single measurement*, Numer. Func. Anal. Opt., 28:519–551, 2007.

[2] H. Ammari, E. Beretta, E. Francini, H. Kang, and M. Lim, *Optimization algorithm for reconstructing interface changes of a conductivity inclusion from modal measurements*, Math. Comp., 79:1757–1777, 2010.

[3] H. Ammari, J. Garnier, V. Jugnon, and H. Kang, *Stability and resolution analysis for a topological derivative based imaging functional*, SIAM J. Control Optim., 50(1):48–76, 2012.

[4] H. Ammari and H. Kang, *Reconstruction of Small Inhomogeneities from Boundary Measurements*, Lectures Notes in Mathematics Series, Springer, 1846, 2004.

[5] M. Bachmayr and M. Burger, *Iterative total variation schemes for nonlinear inverse problems*, Inverse Problems, 25(10):105004, 2009.

[6] S. Baldo, *Minimal interface criterion for phase transitions in mixtures of Cahn-Hilliard fluids*, Ann. IHP Anal. Non Linéaire, 7:67–90, 1990.

[7] E. Beretta, C. Cavaterra, M. C. Cerutti, A. Manzoni, and L. Ratti, *An inverse problem for a semilinear parabolic equation arising from cardiac electrophysiology*, Inverse Problems, 33(10):105008, 2017.

[8] E. Beretta, M. C. Cerutti, A. Manzoni, and D. Pierotti, *An asymptotic formula for boundary potential perturbations in a semilinear elliptic equation related to cardiac electrophysiology*, Math. Mod. Meth. Appl. Sci., 26(04):645–670, 2016.

[9] E. Beretta, E. Francini, and S. Vessella, *Differentiability of the Dirichlet to Neumann map under movements of polygonal inclusions with an application to shape optimization*, SIAM J. Math. Anal., 49(2):756–776, 2017.

[10] E. Beretta, A. Manzoni, and L. Ratti, *A reconstruction algorithm based on topological gradient for an inverse problem related to a semilinear elliptic boundary value problem*, Inverse Problems, 33(3), 2017.

[11] M. Bergounioux and K. Kunisch, *Augemented Lagrangian techniques for elliptic state constrained optimal control problems*, SIAM J. Control Optim., 35(5):1524–1543, 1997.

[12] L. Blank, H. Garcke, C. Hecht, and C. Rupprecht, *Sharp interface limit for a phase field model in structural optimization*, SIAM J. Control Optim., 54(3):1558–1584, 2016.

[13] M. Burger, *Levenberg–Marquardt level set methods for inverse obstacle problems*, Inverse Problems, 20(1):259, 2003.

[14] A. Carpio and M. L. Rapún, *Topological derivatives for shape reconstruction*, in Inverse Problems and Imaging, Springer, 85–133, 2008.

[15] T. F. Chan and X. Tai, *Level set and total variation regularization for elliptic inverse problems with discontinuous coefficients*, J. Comput. Phys., 193(1):40–66, 2004.

[16] C. E. Chávez, N. Zemzemi, Y. Coudière, F. Alonso-Atienza, and D. Alvarez, *Inverse problem of electrocardiography: Estimating the location of cardiac ischemia in a 3D realistic geometry*, International Conference on Functional Imaging and Modeling of the Heart, Springer, 393–401, 2015.

[17] Z. Chen and J. Zou, *An augmented Lagrangian method for identifying discontinuous parameters in elliptic systems*, SIAM J. Control Optim., 37(3):892–910, 1999.

[18] P. G. Ciarlet, M. H. Schultz, and R. S. Varga, *Numerical methods of high-order accuracy for nonlinear boundary value problems*, Numer. Math., 9(5):394–430, 1967.

[19] P. Colli Franzone, L. F. Pavarino, and S. Scacchi, *Mathematical Cardiac Electrophysiology*, MS&A Book Series, Springer, 13, 2014.

[20] K. Deckelnick, C. M. Elliott, and V. Styles, *Double obstacle phase field approach to an inverse problem for a discontinuous diffusion coefficient*, Inverse Problems, 32(4):045008, 2016.

[21] M. C. Delfour and J. P. Zolésio, *Shapes and Geometries: Metrics, Analysis, Differential Calculus and Optimization*, Advances in Design and Control, SIAM, 2011.

[22] G. Dogan, P. Morin, R. H. Nochetto, and M. Verani, *Discrete gradient flows for shape optimization and applications*, Comput. Meth. Appl. Mech. Engineering, 196(37):3898–3914, 2007.

[23] H. W. Engl, M. Hanke, and A. Neubauer, *Regularization of Inverse Problems*, Math. Appl., Springer Netherlands, 1996.

[24] L. C. Evans and R. F. Gariepy, *Measure Theory and Fine Properties of Functions*, CRC press, 2015.

[25] H. Garcke, *The γ-limit of the Ginzburg-Landau energy in an elastic medium*, Adv. Math. Ssci. Appl., 18(2):345–379, 2008.

[26] D. Gilbarg and N. S. Trudinger, *Elliptic Partial Differential Equations of Second Order*, Grundlehren der Mathematischen Wissenschaften. Springer, 1998.

[27] E. Giusti, *Minimal Surfaces and Functions of Bounded Variation*, Springer, 1984.

[28] F. Hettlich and W. Rundell, *The determination of a discontinuity in a conductivity from a single boundary measurement*, Inverse Problems, 14:311–318, 1998.

[29] M. Hintermüller and A. Laurain, *Electrical impedance tomography: from topology to shape*, Control Cybernet., 37(4):913–933, 2008.

[30] V. Isakov, *On uniqueness of recovery of a discontinuous conductivity coefficient*, Comm. Pure Appl. Math., 41(7):865–877, 1988.

[31] R. V. Kohn and M. Vogelius, *Relaxation of a variational method for impedance computed tomography*, Comm. Pure Appl. Math., 40(6):745–777, 1987.

[32] V. Kolehmainen, S. R. Arridge, W. R. B. Lionheart, M. Vauhkonen, and J. P. Kaipio, *Recovery of region boundaries of piecewise constant coefficients of an elliptic PDE from boundary data*, Inverse Problems, 15(5):1375, 1999.

[33] E. H. Lieb and M. Loss, *Analysis*, Second Edition, Graduate Studies in Mathematics, Amer. Math. Soc., 14, 2001.

[34] M. Lysaker, B. F. Nielsen, and A. Tveito, *On the use of the resting potential and level set methods for identifying ischemic heart disease: An inverse problem*, J. Comput. Phys., 220:772–790, 2007.

[35] F. Negri, *redbKIT Version 2.2*, Copyright (c) 2015-2017, Ecole Polytechnique FédFérale de Lausanne (EPFL) All rights reserved, http://redbkit.github.io/redbKIT/, 2016.

[36] J. Nocedal and S. J. Wright, *Numerical Optimization*, Second Edition, Springer, 2006.

[37] L. Rondi and F. Santosa, *Enhanced electrical impedance tomography via the Mumford–Shah functional*, ESAIM Control Optim. Calc. Var., 6:517–538, 2001.

[38] F. Santosa, *A level-set approach for inverse problems involving obstacles*, ESAIM Control Optim. Calc. Var., 1:17–33, 1996.

[39] J. Sundnes, G. T. Lines, X. Cai, B. F. Nielsen, K. A. Mardal, and A. Tveito, *Computing the Electrical Activity in the Heart*, Monographs in Computational Science and Engineering Series, Springer, 1, 2006.

[40] L. Tung, *A bidomain model for describing ischemic myocardial D-C potentials*, MIT, Cambridge, MA, Ph.D. Thesis Edition, 1978.